Quantum materials : fundamentals and applications

From the notes of Professor Gregor Jotzu

Written by Louis Gobber

Spring 2024-2025

Contents

This document reports the notes from the lecture *Quantum materials : fundamentals and applications* of Professor Gregor Jotzu.

Example of NV Centers to Motivate This Field of Research

Applications

NV centers have a wide range of applications in various fields, including quantum technologies and sensing:

- **Fluorescent markers**
- **Single-photon sources**
- **Quantum bits (Qubits)**
- **Quantum memories**
- **Quantum sensors** for:
  - Temperature
  - Strain & pressure
  - Electric and magnetic fields

General Properties of Diamond

Diamond, as a host material for NV centers, possesses exceptional properties:

- Can be **polished**, **laser-cut**, and **RIE etched** (Reactive Ion Etching)
- Can be **grown via CVD** (Chemical Vapor Deposition)
- Can withstand **pressures up to** ~ 500 GPa (5 MBar)
- Thermal stability up to **700°C**
- **High thermal conductivity**: ~ 2000 W/K/m
- **Non-toxic** and **acid-resistant**

How to Generate NV Centers?

NV centers can be created through several methods:

- **Naturally occurring** in some diamonds
- **Introduced during CVD** (Chemical Vapor Deposition) growth
- **Ion implantation** with nitrogen at energies from **2 keV up to 20 MeV**, followed by **annealing at 700°C**
- **Vacancy creation** using **femtosecond (fs) laser pulses**

Chapter 1

Mathematical Basis

1.1 Formalism

To properly describe quantum theory, we must establish the correct mathematical formalism.

First, we define the fundamental quantum states known as "bra" and "ket" vectors. A **ket** represents a state vector in a Hilbert space and is denoted as $|\Psi\rangle$. The **bra** is its corresponding dual vector, written as $\langle\Psi|$, and is obtained via the Hermitian conjugate:

$$c|\Psi\rangle \longrightarrow \langle\Psi|c^*.$$

where c is a complex number.

1.1.1 Projection and Probability Interpretation

To determine the probability of measuring the system in a particular state $|\alpha\rangle$, we use the projection of $|\Psi\rangle$ onto a chosen basis $\{|\alpha\rangle, |\beta\rangle, ...\}$, leading to the probability:

$$P_\alpha = |\langle\alpha|\Psi\rangle|^2.$$

For a valid probability interpretation, the wavefunction must be normalized:

$$\langle\Psi|\Psi\rangle = 1.$$

Additionally, the inner product satisfies the conjugate symmetry property:

$$\langle\alpha|\Psi\rangle = \langle\Psi|\alpha\rangle^*.$$

1.1.2 Two-Dimensional Example

Consider a two-dimensional Hilbert space with an orthonormal basis $\{|0\rangle, |1\rangle\}$, satisfying:

$$|\langle 0|1\rangle|^2 = 0, \quad \text{or more generally,} \quad |\langle i|j\rangle|^2 = \delta_{i,j}.$$

A practical example is the polarization of light, where the horizontal and vertical polarization states form the basis:

$$\{|H\rangle, |V\rangle\}.$$

Here, $|H\rangle$ represents horizontal polarization and $|V\rangle$ vertical polarization. The superposition states correspond to diagonal polarizations:

$$|+\rangle = \frac{1}{\sqrt{2}}(|H\rangle + |V\rangle), \quad |-\rangle = \frac{1}{\sqrt{2}}(|H\rangle - |V\rangle).$$

Circular polarization states are given by:

$$|R\rangle = \frac{1}{\sqrt{2}}(|H\rangle + i|V\rangle), \quad |L\rangle = \frac{1}{\sqrt{2}}(|H\rangle - i|V\rangle).$$

Another common example is the **spin-$\frac{1}{2}$** system, where the standard basis is:

$$\{|\uparrow\rangle, |\downarrow\rangle\}$$

and the superposition states are:

$$|\rightarrow\rangle = \frac{1}{\sqrt{2}}(|\uparrow\rangle + |\downarrow\rangle), \quad |\leftarrow\rangle = \frac{1}{\sqrt{2}}(|\uparrow\rangle - |\downarrow\rangle).$$

1.1.3 Wavefunction Decomposition

A general wavefunction can be expressed in a chosen basis as:

$$|\Psi\rangle = c_0|0\rangle + c_1|1\rangle.$$

Using a phase convention, this can be rewritten as:

$$|\Psi\rangle = e^{i\Phi_0}\left(a_0|0\rangle + a_1 e^{i(\Phi_1 - \Phi_0)}|1\rangle\right),$$

where Φ_0 is the **global phase**, a_0 and a_1 are real coefficients, and the normalization condition imposes:

$$\langle\Psi|\Psi\rangle = a_0^2 + a_1^2 = 1.$$

1.2 Bloch Sphere Representation

A two-level quantum system can be conveniently represented on the **Bloch sphere**, where any pure state can be written as:

$$|\Psi\rangle = \cos\frac{\theta}{2}|0\rangle + e^{i\phi}\sin\frac{\theta}{2}|1\rangle.$$

Here, θ and ϕ define the position of the state on the sphere, with $\theta \in [0; \Pi]$ and $\Phi \in [0; 2\Pi]$.

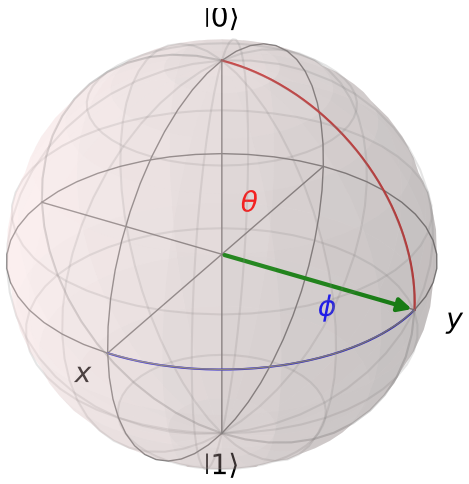

Figure 1.1: Bloch sphere. $|0\rangle$ and $|1\rangle$ are the two states of the system. The plane $\{x, y\}$ corresponds to a real phase.

1.3 Unitary Operators, Schrödinger Equation, and Hamiltonian

The most general form of any **2D Hamiltonian** is given by:

$$\hat{H} = h_0\mathbb{I} + h_x\hat{\sigma}_x + h_y\hat{\sigma}_y + h_z\hat{\sigma}_z,$$

where the **Pauli matrices** are:

$$\sigma_x = \begin{pmatrix} 0 & 1 \\ 1 & 0 \end{pmatrix}, \quad \sigma_y = \begin{pmatrix} 0 & -i \\ i & 0 \end{pmatrix}, \quad \sigma_z = \begin{pmatrix} 1 & 0 \\ 0 & -1 \end{pmatrix}.$$

Since $\hat{H}$ is Hermitian, its eigenvalues are:

$$\varepsilon_{0,1} = h_0 \pm \sqrt{h_x^2 + h_y^2 + h_z^2} = h_0 \pm |h|,$$

where $|h| = \sqrt{h_x^2 + h_y^2 + h_z^2}$.
The corresponding eigenvectors are:

$$|\psi_0\rangle = \begin{pmatrix} \cos\frac{\pi-\theta}{2} \\ \sin\frac{\pi-\theta}{2}e^{-i\phi} \end{pmatrix}, \quad |\psi_1\rangle = \begin{pmatrix} \cos\frac{\theta}{2} \\ \sin\frac{\theta}{2}e^{i\phi} \end{pmatrix}.$$

1.3.1 Unitary Time Evolution Operator

The unitary time evolution operator governs the time evolution of a quantum state under a Hamiltonian $\hat{H}$. It is given by:

$$\hat{U} = e^{-i\hat{H}t/\hbar} = \cos\left(\frac{|h|t}{\hbar}\right)\mathbb{I} + i\sin\left(\frac{|h|t}{\hbar}\right)\frac{\vec{h}\cdot\vec{\sigma}}{|h|}$$

where:

$$\vec{h} = (h_x, h_y, h_z), \quad \vec{\sigma} = (\sigma_x, \sigma_y, \sigma_z).$$

1.3.2 Properties of the Evolution Operator

The unitary evolution operator satisfies the unitarity condition:

$$\hat{U}^\dagger \hat{U} = \mathbb{I}$$

which ensures that quantum evolution is **norm-preserving** and **reversible**.

1.3.3 Rotation on the Bloch Sphere

The decomposition of $\hat{U}$ reveals that the quantum evolution corresponds to a **rotation** of the state vector on the Bloch sphere:

$$\hat{U} = e^{-i\frac{|h|t}{\hbar}\hat{n}\cdot\vec{\sigma}} = \cos\left(\frac{|h|t}{\hbar}\right)\mathbb{I} - i\sin\left(\frac{|h|t}{\hbar}\right)(\hat{n}\cdot\vec{\sigma}).$$

where $\hat{n} = \frac{\vec{h}}{|h|}$ is the unit vector along $\vec{h}$, meaning the evolution is a **rotation by angle $\theta = \frac{2|h|t}{\hbar}$ about axis $\hat{n}$**.

1.3.4 Action on a Quantum State

For an arbitrary quantum state $|\psi(0)\rangle$, the evolved state at time t is:

$$|\psi(t)\rangle = \hat{U}|\psi(0)\rangle.$$

If the initial state is an eigenstate of $\hat{H}$, the time evolution simply introduces a phase factor:

$$\hat{U}|\psi_i\rangle = e^{-iE_i t/\hbar}|\psi_i\rangle.$$

For a **superposition state**, the time evolution results in a phase accumulation and a mixing of states depending on $\hat{H}$.

1.3.5 Example: Evolution of a Spin-1/2 System in a Magnetic Field

Consider a spin-1/2 particle in a magnetic field along the z-axis. The Hamiltonian is:

$$\hat{H} = \frac{\hbar\omega}{2}\sigma_z.$$

The unitary time evolution operator is then:

$$\hat{U}(t) = e^{-i\frac{\omega t}{2}\sigma_z} = \begin{pmatrix} e^{-i\frac{\omega t}{2}} & 0 \\ 0 & e^{i\frac{\omega t}{2}} \end{pmatrix}.$$

This describes a phase evolution of the spin-up and spin-down states.

1.3.6 Infinitesimal Evolution and the Schrödinger Equation

Expanding $\hat{U}$ for small t:

$$\hat{U}(t) \approx \mathbb{I} - \frac{i}{\hbar}\hat{H}t + O(t^2).$$

This leads directly to the **time-dependent Schrödinger equation**:

$$i\hbar\frac{d}{dt}|\psi(t)\rangle = \hat{H}|\psi(t)\rangle.$$

1.3.7 Connection to Quantum Gates

In quantum computing, unitary evolution corresponds to a quantum gate:

- If $\hat{H} \propto \sigma_x$, then $\hat{U}$ acts as an **X-rotation gate**. - If $\hat{H} \propto \sigma_y$, then $\hat{U}$ acts as a **Y-rotation gate**. - If $\hat{H} \propto \sigma_z$, then $\hat{U}$ acts as a **Z-rotation gate**.

These are fundamental operations in **quantum computing** and quantum information processing.

Chapter 2

NV centers and population transfer

2.1 Photoluminescence Properties of NV Centers

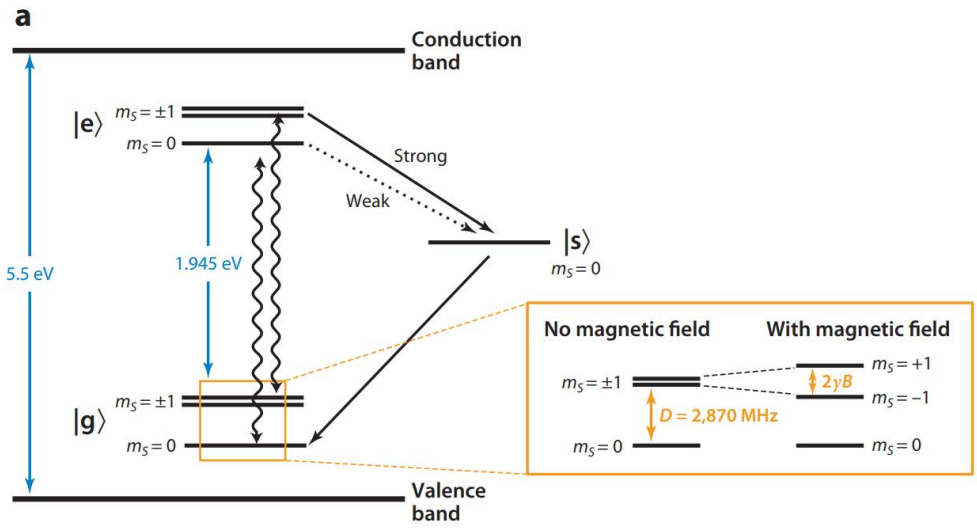

Figure 2.1: Energy diagram of NV centers. The ground state is splitted by the Zero field splitting and optical pumping is possible. (From Annu. Rev. Phys. Chem. 2014. 65:83–105, *Schirhagl et al.*)

Nitrogen-Vacancy (NV) centers exhibit remarkable **photoluminescence** properties, which, as you will see, make them highly effective for detection purposes.

These centers are **optically pumped** using a **green laser** with a wavelength between 515 nm and 532 nm. Following excitation, they emit **fluorescence** over a broad range of 600 nm to 700 nm, with a characteristic peak at 637 nm.

2.1.1 Triplet Ground and Excited States

We focus on the case of the **triplet ground state** ^3G (denoted $|g\rangle$), which is optically excited to the **triplet excited state** ^3E (denoted $|e\rangle$). The relaxation back to the

ground state occurs via two possible pathways:

- **Radiative decay**: Direct fluorescence emission.
- **Non-radiative decay**: A transition through a **metastable state**, which is more probable if the NV center is in the $m_s = \pm 1$ **state**.

This spin-dependent decay mechanism is crucial: it creates a fluorescence **contrast** between different spin states, enabling **optical readout** of the spin state. This property makes NV centers highly valuable for quantum sensing applications.

2.1.2 Fluorescence Collection

A single NV center can emit up to 1×10^6 photons per second, making it detectable with the right optical setup, such as **parabolic collectors** or high numerical aperture objectives.

2.2 Zero-Field Splitting and Microwave Control

In the absence of an external magnetic field, the NV center's triplet ground state consists of:

- A singlet state $m_s = 0$, and
- A degenerate doublet $m_s = \pm 1$.

These states are separated by a well-known **zero-field splitting** of:

$$D = 2.87\,\text{GHz}. \tag{2.1}$$

This means that the $m_s = \pm 1$ states can be selectively populated by applying **microwave (MW) radiation** at the resonance frequency.

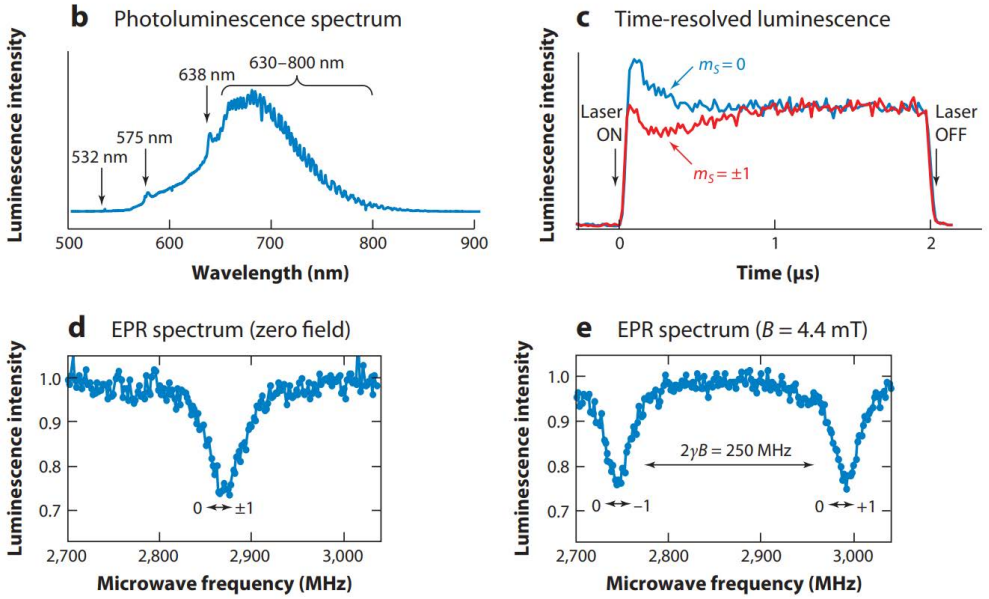

Figure 2.2: Spectrum and fluorescence properties of NV centers (From Annu. Rev. Phys. Chem. 2014. 65:83–105, *Schirhagl et al.*)

2.3 Spin State Initialization

The excited state $|e\rangle$ has a finite lifetime:

- **Bulk diamond**: ~ 13 ns,
- **Nanodiamonds**: Up to 25 ns.

The ground state $|g\rangle$ has a **longer lifetime** (on the order of milliseconds). This allows efficient **spin initialization**:

- When MW excitation stops, applying **green light** for a few milliseconds optically pumps the system back into the $m_s = 0$ state.

This mechanism provides a reliable way to **prepare and control the spin state** of the NV center.

2.4 Magnetic Field Sensing

Applying an external **magnetic field** B lifts the degeneracy of the $m_s = \pm 1$ states, causing a Zeeman splitting given by:

$$\Delta E = 2\gamma|B| = 2 \times (28\,\mathrm{GHz/T}) \times |B|. \tag{2.2}$$

This shift allows NV centers to function as **highly sensitive magnetometers**. By tuning the applied **microwave frequency** and observing fluorescence contrast, we can precisely measure external magnetic fields.

(see figure 2.2).

2.5 Quantum sensing and population transfer

NV centers are mainly used as quantum sensors for detecting low magnetic fields. The technique is generally called ODMR for "Optically Detected Magnetic Resonance" or also "Optical ESR". As we explained earlier, the presence of a magnetic field will add a Zeeman term to the Hamiltonian, and help us to resolve two peaks on the resonancy curve.

Sensitivity of ODMR

$$\Delta\omega = 2\gamma B = \frac{HWHM}{2\eta\sqrt{N_{photons}}} \approx 10kHz/\sqrt{Hz} \approx nT/\sqrt{Hz} \tag{2.3}$$

Now, when applying a DC magnetic field, we can choose to look at the system as a two-level system between the states $m_s = 0$ and $m_s = -1$. In this representation, $H = h_z\sigma_z$, and if we start from $|\Psi_0 >= |\uparrow>$, how can we rotate the spin state to the state $|\Psi(t) >= |\downarrow>$?

Brute force

The first possibility is to apply a strong magnetic field; however, it means an order of magnitude of the tesla range, which is hard to obtain experimentally.

The Hamiltonian would looks like :

$$H = h_x\sigma_x + h_z\sigma_z \tag{2.4}$$

with $h_x >> h_z$.

Example taking h_x=20h_z :

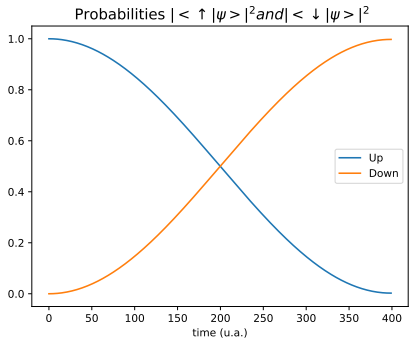

(a) Population Transfer

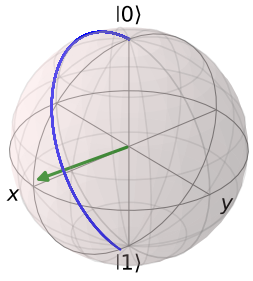

(b) Bloch sphere representation

Figure 2.3: Using a hard pulse to switch state

What is interesting to notice is that in this configuration the eigenstate is not exactly on the x-axis but a bit off. Then the population transfer is not complete. To obtain a proper $\frac{\Pi}{2}_X$ pulse, one has to apply a Hamiltonian without $_Z$ component.

Resonant transfer

A **resonant transfer** is possible for smaller amplitudes of the magnetic field. The only condition for successfully transferring the spin state is a **matching frequency** (Rabi frequency). The Hamiltonian in this case is time-dependent, but we do not require slowly varying eigenstates:

$$\hat{H}(t) = h_x(t)\sigma_x + h_z\sigma_z = h_x \sin(\omega t)\sigma_x + h_z\sigma_z. \tag{2.5}$$

When the driving field is weak compared to the static field, i.e.,

$$h_x \ll h_z, \tag{2.6}$$

the energy splitting between eigenstates is given by and the frequency ω_0 of the excitation does match this energy difference in order to make the resonant transfer possible:

$$\epsilon_+ - \epsilon_- = 2\sqrt{h_x^2 + h_z^2}. \tag{2.7}$$

If you change the frequency slighlty off ω_0, you can not get a complete population transfer. This situation is often visualized using the **peeled orange representation**, where the Bloch sphere appears divided into slices, illustrating the oscillation of the quantum state under a weak driving field. This representation highlights the trajectory of the quantum state as it transitions under the influence of the oscillating field.

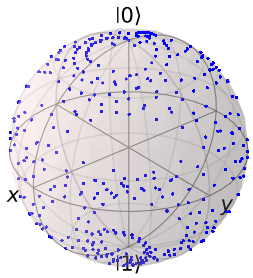

(a) Resonant transfer

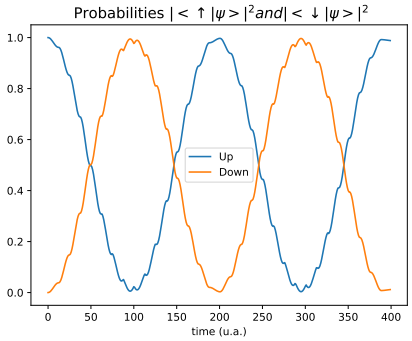

(b) Population evolution for a resonant transfer

Figure 2.4: Using a resonant transfer to switch state

Adiabatic transfer

Finally, an "adiabatic transfer" corresponds to changing eigenstates which vary slowly enough to go from one state to another. In that case the Hamiltonian depends on time like:

$$H = h_x(t)\sigma_x + h_z(t)\sigma_z \tag{2.8}$$

$|\Psi(t) >$ follows closely the eigenstate and takes the same path around the Bloch sphere, and this is not really feasible experimentally :

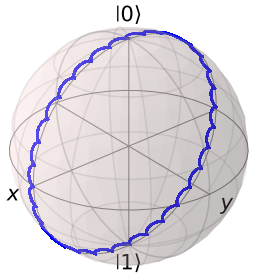

(a) Adiabatic transfer

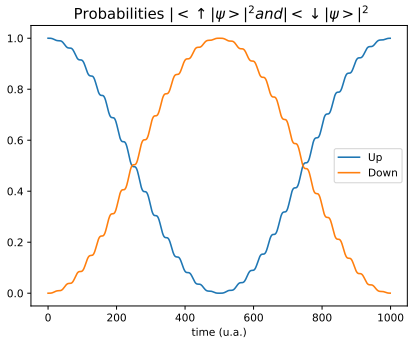

(b) Population evolution for an adiabatic transfer

Figure 2.5: Using an adiabatic transfer to switch state

Until now we took the example of NV centers to present two-level interactions (i.e. the Hamiltonians are 2x2 matrices). However, we should not forget that the NV centers have a degenerate excited state for $| \pm 1 >$. In order to consider a two-level excitation, a DC magnetic field can be used to split these levels.

2.6 NV centers : a 3-level system

NV centers have a spin 1 and to describe the interactions of the spin we now need 3x3 Hamiltonian and spin operator matrices. The Hamiltonian of NV centers in diamond depends on the system's specific configuration, but the general simplified Hamiltonian is :

$$H_{NV} = DS_Z^2 + g\mu_B B \cdot S \tag{2.9}$$

Spin-1 operators can be defined :

$$S_x = \begin{bmatrix} 0 & 1 & 0 \\ 1 & 0 & 1 \\ 0 & 1 & 0 \end{bmatrix}; S_y = \begin{bmatrix} 0 & -i & 0 \\ i & 0 & -i \\ 0 & i & 0 \end{bmatrix}; S_z = \begin{bmatrix} 1 & 0 & 0 \\ 0 & 0 & 0 \\ 0 & 0 & -1 \end{bmatrix} \tag{2.10}$$

Around 75mT we see that levels $|0\rangle$ and $|-1\rangle$ do cross, we can basically expect an eigenstate of the shape $|\rightarrow\rangle$ if we consider the two-level system $\{|0\rangle, |-1\rangle\}$

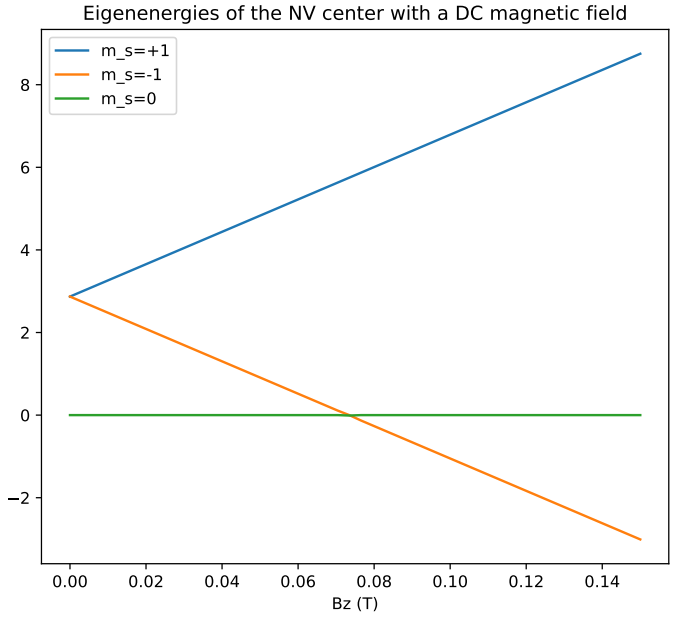

Figure 2.6: NV center energy levels with a DC magnetic field along the NV axis. The energy scale is given in GHz

We are not able to represent a 3-level system on the Bloch sphere, though, it is possible to project two states on the good spin-operator matrices and partially represent the interactions of two of the three levels of the system...

Chapter 3

Tight Binding model and Geometric phase

3.1 From two-state system to a chain of sites

3.1.1 Two-level system

Two-state system simpliest representation:

$$H = \frac{\Delta}{2}\sigma_z \tag{3.1}$$

Eigenstates:

$$E = \pm\frac{\Delta}{2}, \quad |\uparrow\rangle, |\downarrow\rangle \tag{3.2}$$

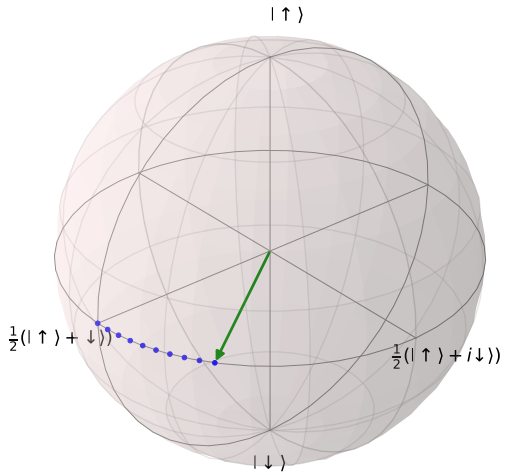

Figure 3.1: Two level system without tunneling

Now let's add hopping terms and we do not consider the σ_z term (case $\Delta = 0$), but pay attention, H_t must be Hermitian (meaning we have time-reversal symmetry):

$$H_t = -t(a_\uparrow^\dagger a_\downarrow + a_\downarrow^\dagger a_\uparrow) \tag{3.3}$$

$a_\uparrow$ and $a_\downarrow$ are, respectively, the creation and anihilation operators, t is an energy but corresponds to the tunneling probability.

If $|\Psi_0\rangle = |\uparrow\rangle$ the corresponding transfer period is $\tau_{\uparrow\downarrow} = \frac{\Pi\hbar}{2t}$. On the Energy graph we expect two points at $\pm t$.

3.1.2 Chain of sites and momentum basis

Now, let's increase the number of sites considering a chain of sites, that could be a dicoupled diatomic chain :

$$H = \sum_{j=0}^{N-1} (-1)^j \frac{\Delta}{2} a_j^\dagger a_j - t \sum_{j=0}^{N-2} (a_{j+1}^\dagger a_j + a_j^\dagger a_{j+1}) \tag{3.4}$$

Even sites will have an onsite energy $+\frac{\Delta}{2}$ and odd sites $-\frac{\Delta}{2}$. The index for the hopping term goes from zero to N-2 because we are not considering circular boundary conditions for now, and a tunneling at the end of the chain is not possible. If you want the circularity, just change the final index to N-1.

The best way to understand the hamiltonian is actually to plot it. What you see are the diagonal terms coming from on-site energies and off diagonal are the hopping terms which links neighboor sites. When adding circular boundary conditions you see appearing those two supplementary terms off diagonal connecting the first and last sites.

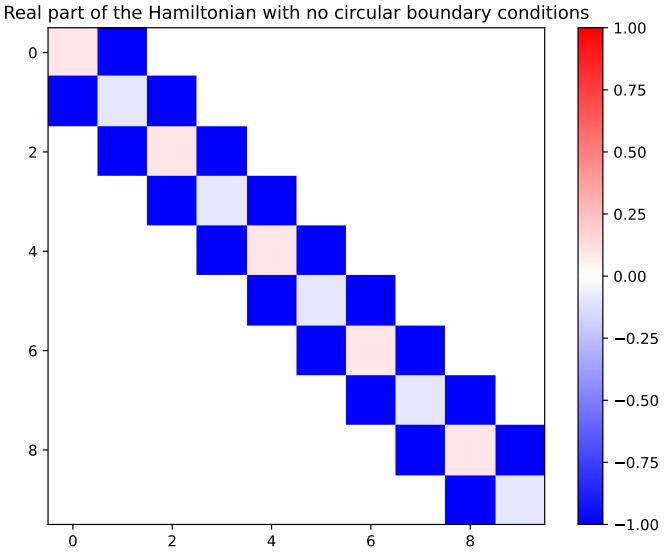

Figure 3.2

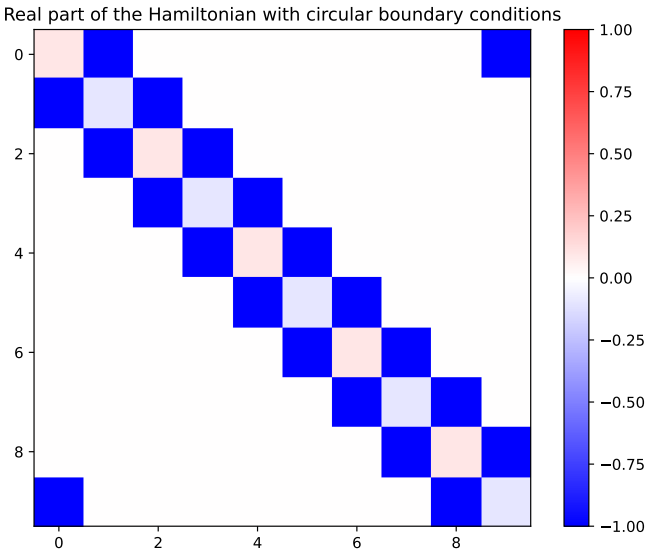

Figure 3.3

Now we understand what is the real space Hamiltonian, let's look a the wavefunction distribution for given eigenstates and the energy spectrum:

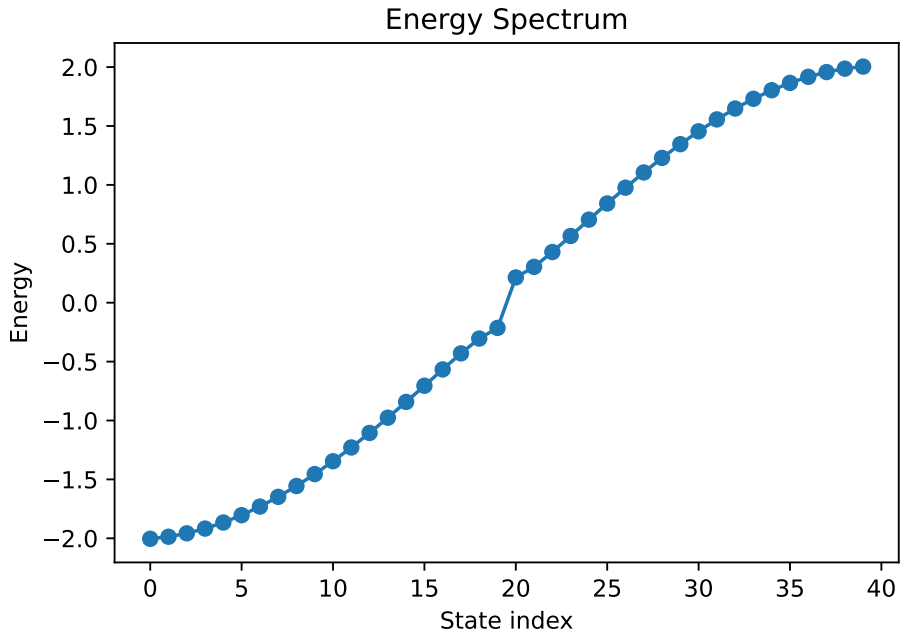

Figure 3.4: No circular boundary conditions

If we do plot the eigenergies in the real space, we can see the cosinusoidal shape of the energy distribution. Both cosine curves have an amplitude of 2t (where t=1), and

we see an opened gap of $\Delta = 0.4$. More visibly, we can look at the distribution of the wavefunction for some eigenstates of the system :

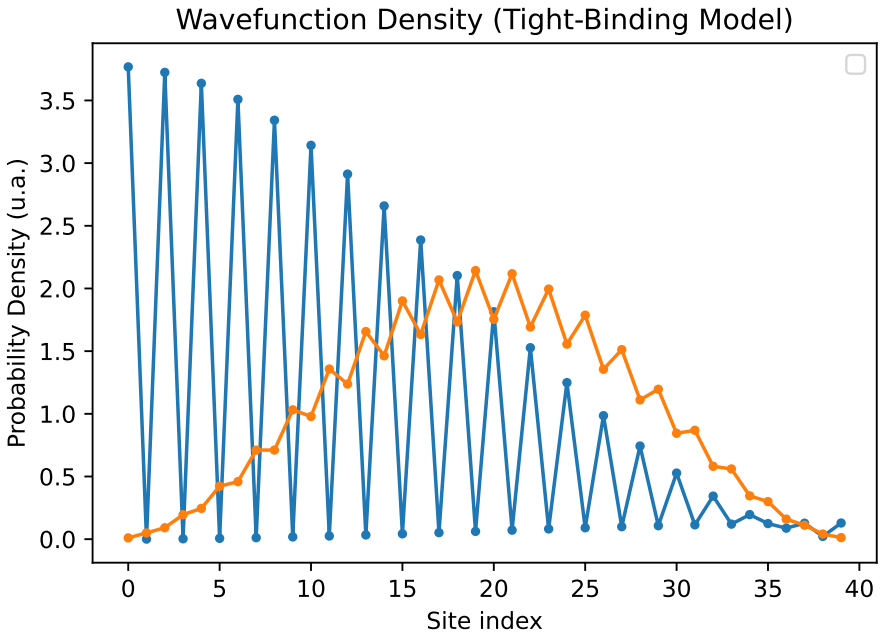

Figure 3.5: Wavefunction localization for two of the eigenstates

What has to be noticed is first, the presence of those edge states that will disappear if we had circular boundary conditions because they represent states localized at the edges. Also, you can not find flat standing wavefunctions of 0 energy without circular boundary conditions, it would cost to much in Energy for the wavefunction to drop to 0 on the edges. This mean that if we set $\Delta = 0$, you will see eigenenergies states in the gap only with circulary boundary conditions.

Adding circular boundary conditions should change those characteristics:

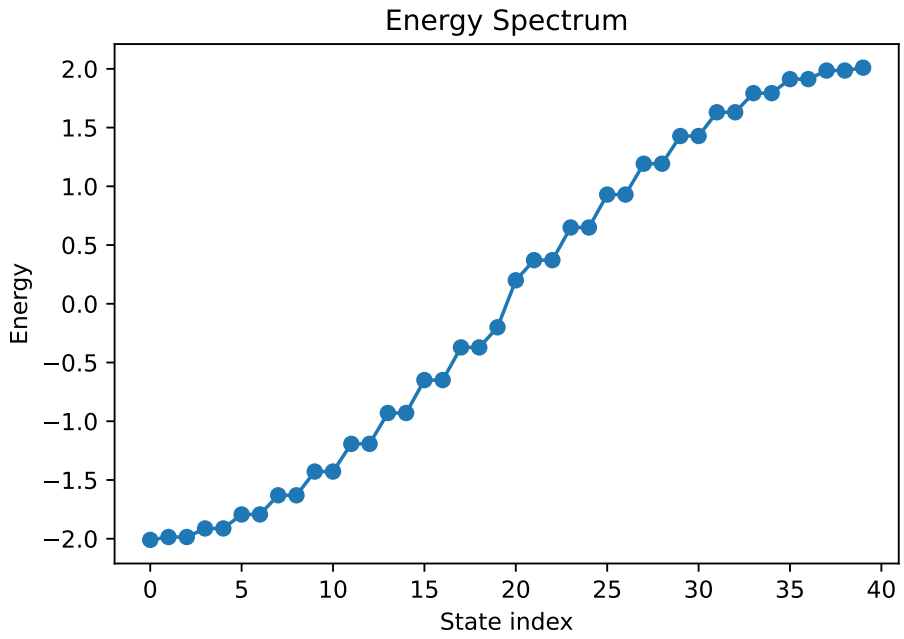

Figure 3.6: Circular boundary conditions

Eigenergies are now paired and the pairing comes from the fact that we can find two different eigenstates of same eigenenergy but opposite momentum.

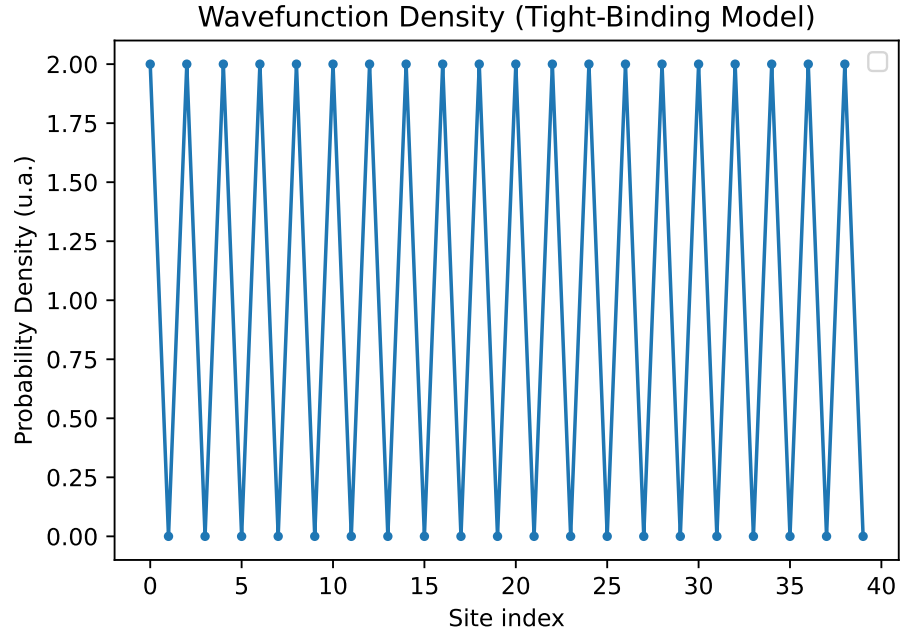

Figure 3.7: Wavefunction localization for two of the eigenstate with circular boundary conditions

In those plots, it is clear that the basis of states is the basis $\{|j\rangle\}$ where j are the different sites as every eigenstates are localized exactly on the sites. However, it is preferable to work in the momentum basis to plot the band structures. For this we need to change of basis and the usual wavefunction expansion is :

$$|k\rangle = \frac{1}{\sqrt{N}} \sum_j e^{ik\cdot j} |j\rangle \tag{3.5}$$

still conserving the orthogonality condition:

$$\langle k'|k\rangle = \delta_{kk'} \tag{3.6}$$

The Hamiltonian looks now completely different :

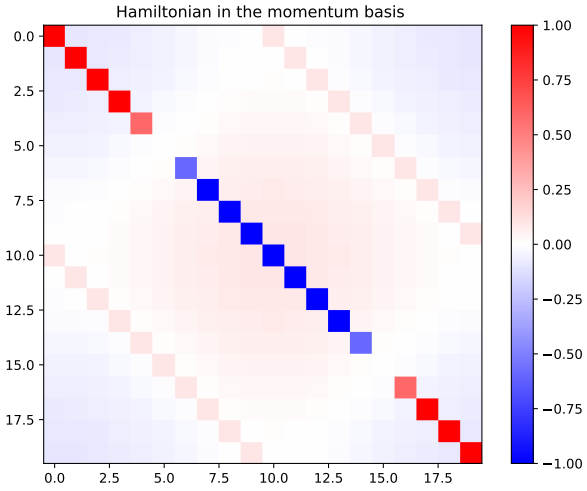

Figure 3.8

In the momentum space representation, we are going to plot the eigenenergies over a given period which could be either $[-\frac{\pi}{a}, \frac{\pi}{a}]$ or $[0, \frac{2\pi}{a}]$. The discretisation of k depends on the total number of sites N; $\frac{2\pi}{Na}$, meaning that a bigger number of sites looks like a continuum on the Energy spectrum.

In the k-space, the hopping Hamiltonian would then be :

$$H_t = -t \sum_k 2\cos(ka)|k\rangle\langle k| \tag{3.7}$$

And the band structure representation:

$$E_k = -2t\cos(ka) \tag{3.8}$$

3.2 SSH model

The SSH model was first introduced in order to model polyacethylene. It does correspond to the same kind of 1D chain, but now with different tunneling probabilities between sites.

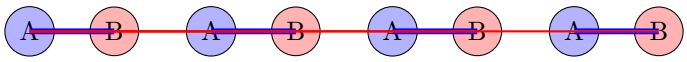

The Hamiltonian of the system is given by :

$$H = \sum_j \left[-t_1(a_j^\dagger b_j + b_j^\dagger a_j) - t_2(a_{j+1}^\dagger b_j + b_j^\dagger a_{j+1}) \right] + \frac{\Delta}{2} a_j^\dagger a_j - \frac{\Delta}{2} b_j^\dagger b_j \tag{3.9}$$

Using the proper base $|a,k\rangle$ and $|b,k\rangle$, the Hamiltonian can be written as a matrix like :

$$H = \begin{pmatrix} \frac{\Delta}{2} & -t_1 - t_2 e^{-ika} \\ -t_1 - t_2 e^{ika} & -\frac{\Delta}{2} \end{pmatrix} \tag{3.10}$$

Components of H :

$$H_x = -(t_1 + t_2)\cos(ka)\sigma_x \tag{3.11}$$
$$H_y = -(t_1 - t_2)\sin(ka)\sigma_y \tag{3.12}$$
$$H_z = \frac{\Delta}{2}\sigma_z \tag{3.13}$$

The energy is given by:

$$E = \pm\sqrt{h_x^2 + h_y^2 + h_z^2} \tag{3.14}$$

3.3 Tight-Binding Approximation for Graphene

3.3.1 Hamiltonian

The tight-binding Hamiltonian is given by:

$$H = \sum_k h(\overrightarrow{K})$$

where the summation is over nearest neighbors so that :

$$H = h_x\sigma_x + h_y\sigma_y = \begin{pmatrix} 0 & \sum_i -t_i e^{-i\overrightarrow{v_i}\cdot\overrightarrow{k}} \\ \sum_i -t_i e^{i\overrightarrow{v_i}\cdot\overrightarrow{k}} & 0 \end{pmatrix} \tag{3.15}$$

with, $|v| = a = 1.42\mathring{A}$ and $t_i \approx 2.8eV$, a being the lattice vector.
The energy dispersion relation is:

$$E = \pm t\sqrt{3 + f(\mathbf{k})}$$

where:

$$f(\mathbf{k}) = 2cos(\sqrt{3}k_y a) + 4cos(\frac{\sqrt{3}}{2}k_y a)cos(\frac{3}{2}k_x a)$$

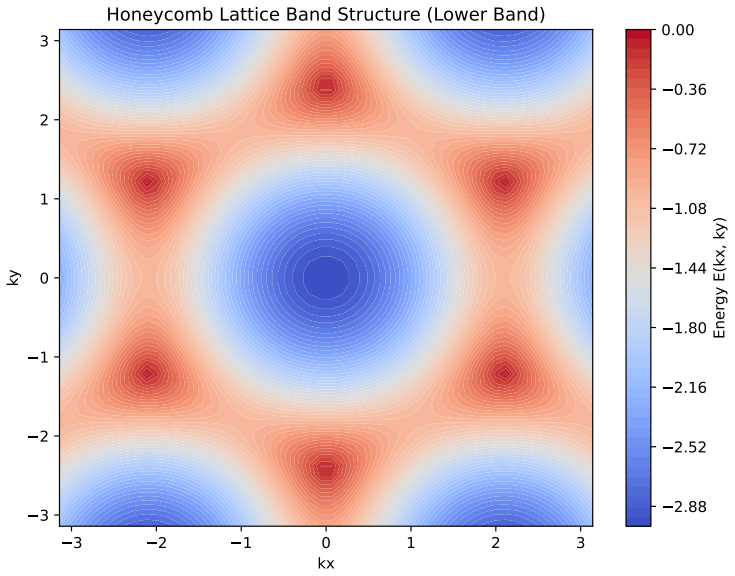

Figure 3.9

Upper and lower bands are completely symmetric when the hopping term is the same between each nearest neighbors.

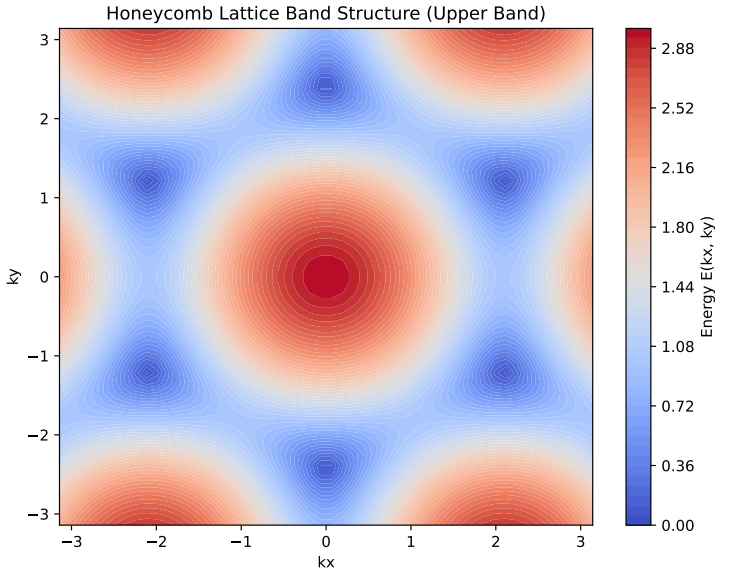

Figure 3.10

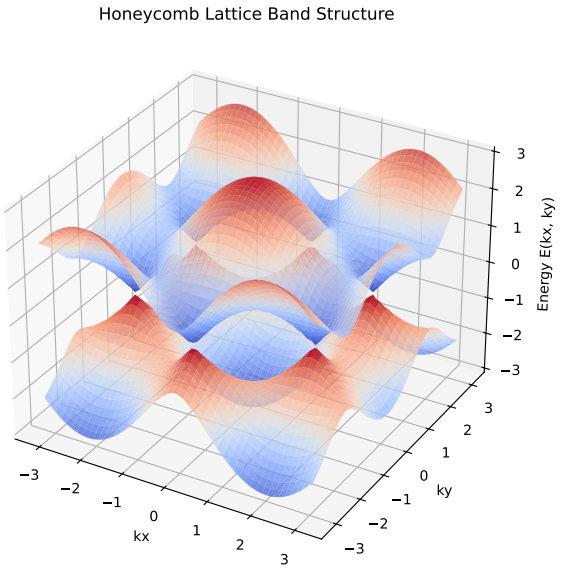

Figure 3.11: 3D representation of the band structure

3.3.2 Key properties

At $\Gamma(0,0)$ point, the energy difference is maximum : $\Delta E = 6t$, "not frustrated". The Dirac points are located at:

$$\mathbf{K} = \left(\frac{2\pi}{3a}, \frac{2\pi}{3\sqrt{3}a}\right), \quad \mathbf{K}' = \left(\frac{2\pi}{3a}, -\frac{2\pi}{3\sqrt{3}a}\right)$$

and you can find other K,K' periodically, for example:

$$\mathbf{K} = \left(0, \frac{4\pi}{3\sqrt{3}a}\right), \quad \mathbf{K}' = \left(0, -\frac{4\pi}{3\sqrt{3}a}\right)$$

Expanding around the Dirac points, we obtain the low-energy Hamiltonian:

$$H_{\text{eff}} = v_F(\sigma_x k_x + \sigma_y k_y)$$

where $v_F = \frac{3ta}{2}$ is the Fermi velocity, $\approx 10^6 m.s^{-1} \approx \frac{c}{300}$

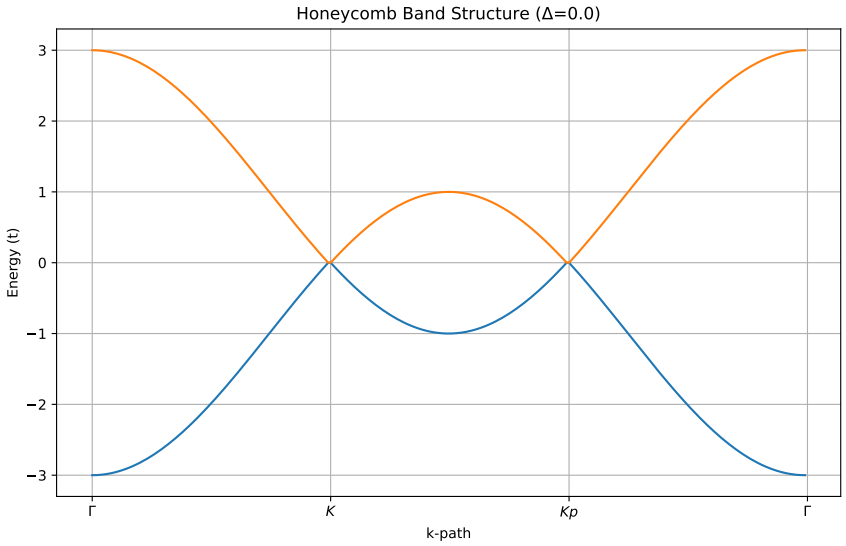

Figure 3.12: K path for a honeycomb lattice. Two Dirac points are distinguishable.

Opening the gaps

We can act on the parameters of our honeycomb lattice to try to open gaps at the Dirac points for instance. This can be achieved by modifying one of the three hopping terms, let's say **t3**.

Down here **t3** is small compared to the other hopping terms, and the direct consequence is the appearing of a preferential direction for conductive channels. The electrons travel easily between sites connected by t1 and t2 hopping terms:

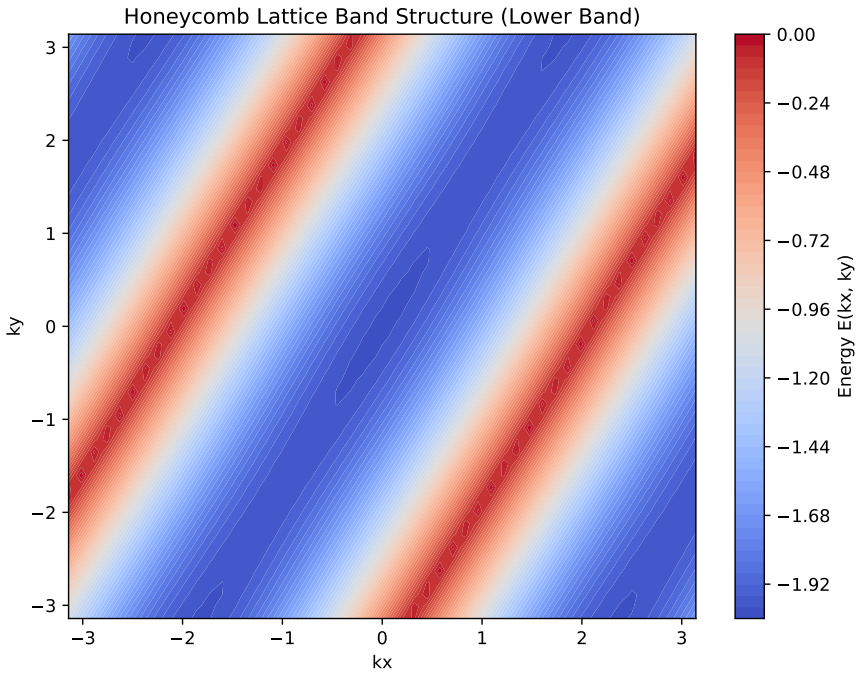

Figure 3.13: Band structure with one smaller hopping term

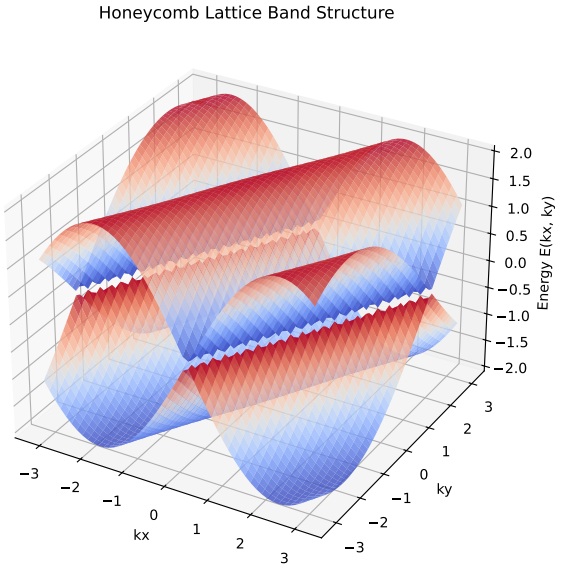

Figure 3.14: 3D representation of the band structure with one smaller hopping term

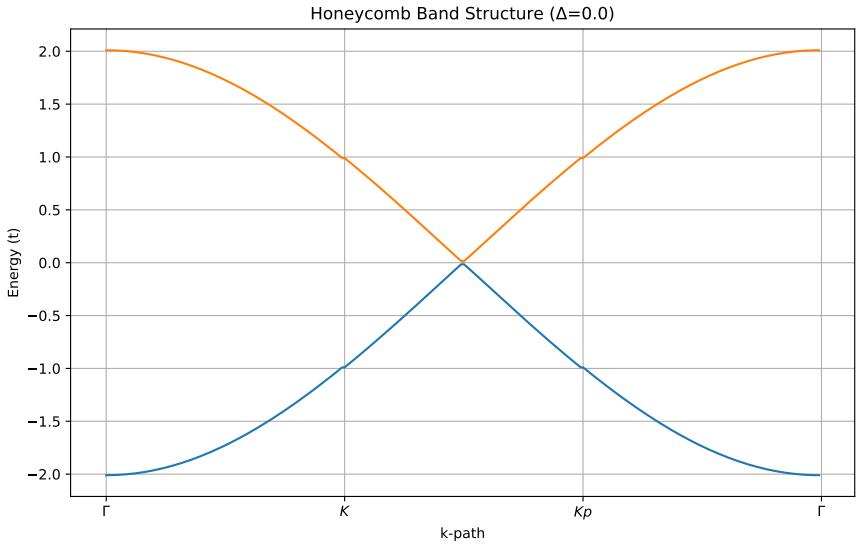

Figure 3.15: K-path with one smaller hopping term

On the contrary, when one of the hopping terms is way bigger than the two others we do obtain opened gaps where were the Dirac points.

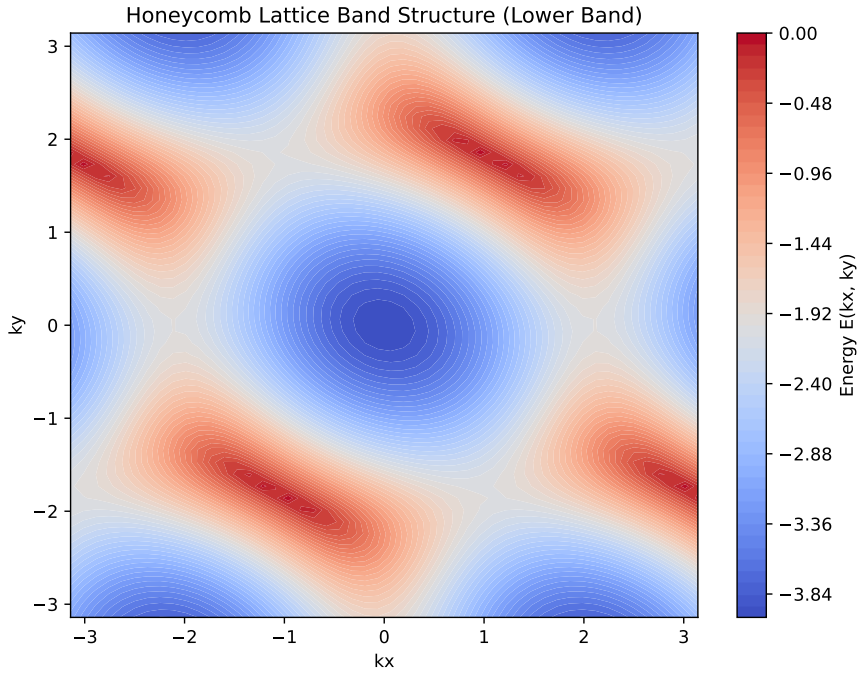

Figure 3.16: Band structure with one bigger hopping term

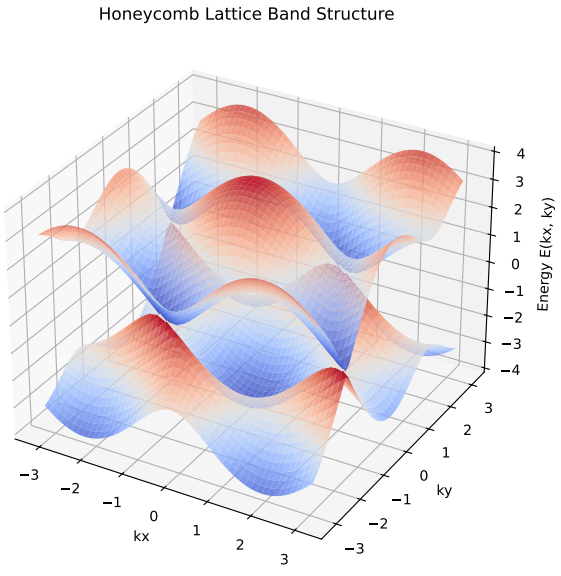

Figure 3.17: 3D Band structure with one smaller hopping term

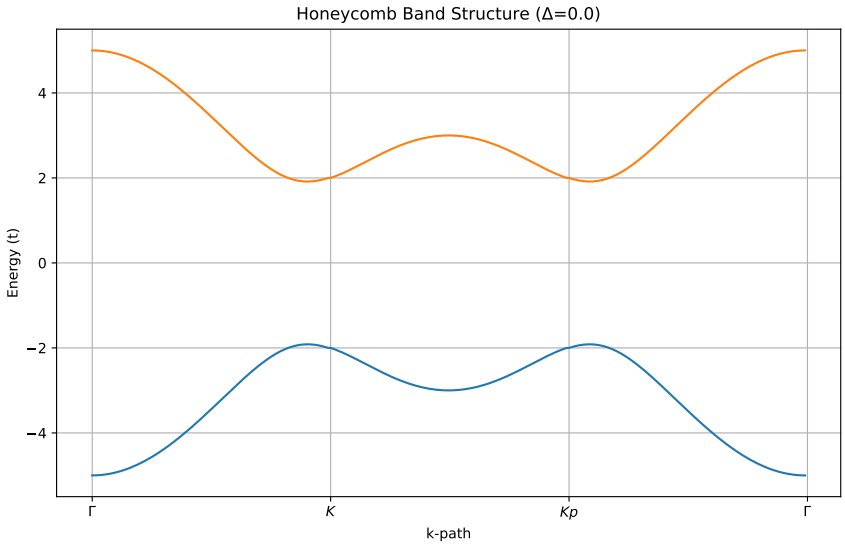

Figure 3.18: K path with one smaller hopping term

One can also try with non zero on-site energy difference Δ.

3.3.3 Symmetry considerations

We now analyze the symmetry properties of the Hamiltonian under key transformations. One has to remember that we will always have:

- $h(K) = h_x\sigma_x + h_y\sigma_y$ with $h_z = 0$ because of $\mathcal{T}$ and $\mathcal{P}$ symmetries in pristine graphene.

- $E(K) = E(-K)$ if we have either $\mathcal{T}$ or $\mathcal{P}$ or both of them.

Time-Reversal Symmetry ($\mathcal{T}$) Time-reversal acts as:

$$\mathcal{T}H(\mathbf{k})\mathcal{T}^{-1} = H(-\mathbf{k})$$

In terms of Pauli matrices, time-reversal is represented by:

$$\mathcal{T} = i\sigma_y\mathcal{K}$$

where $\mathcal{K}$ is complex conjugation. This transformation flips momentum $\mathbf{k} \to -\mathbf{k}$ and also changes the sign of σ_y, leading to:

$$H_{\text{eff}}(-\mathbf{k}) = v_F(-\sigma_x k_x - \sigma_y k_y)$$

which confirms that time-reversal symmetry is preserved.

Inversion Symmetry ($\mathcal{P}$)

Inversion symmetry acts as:

$$\mathcal{P}H(\mathbf{k})\mathcal{P}^{-1} = H(-\mathbf{k})$$

In graphene, inversion exchanges the two sublattices (A and B), which is represented by the Pauli matrix σ_x:

$$\mathcal{P} = \sigma_x$$

Applying inversion to the effective Hamiltonian:

$$\mathcal{P}H_{\text{eff}}(\mathbf{k})\mathcal{P}^{-1} = v_F(\sigma_x k_x + \sigma_y k_y)$$

Since $H_{\text{eff}}(-\mathbf{k}) = v_F(-\sigma_x k_x - \sigma_y k_y)$, inversion symmetry is respected.

Combined $\mathcal{PT}$ Symmetry

The combination of time-reversal and inversion acts as:

$$\mathcal{PT} = \sigma_x(i\sigma_y\mathcal{K}) = i\sigma_z\mathcal{K}$$

which satisfies:

$$(\mathcal{PT})^2 = -1$$

indicating a Kramers degeneracy, which protects the Dirac points from being gapped unless additional symmetry-breaking terms are introduced.

The Dirac points are protected by time-reversal and inversion symmetry:

$$\mathcal{PT} = -1$$

This ensures that the gap remains closed unless a perturbation breaks symmetry.

3.4 Geometric phase

For any trajectory in K-space:

$$|\Psi(\overrightarrow{K}(0))> \rightarrow e^{i\Theta_{tot}}|\Psi(\overrightarrow{K}(t))>$$

and

$$\overrightarrow{K}(0) = \overrightarrow{K}(t).$$

Where:

$$\Theta_{tot} = \frac{1}{\pi}\int_0^t <\Psi|H|\Psi> dt' - \int_0^t <\Psi|\partial_t|\Psi> dt'.$$

The first term here is the "Dynamical phase" which is like asking ourselves the question " for how long are we doing the loop?". The second term is the so-called Geometric phase or AA phase noted β.

Dynamical Phase and Adiabatic Effects

The total phase accumulated by a wavefunction evolving in time is:

$$\theta_{\text{total}} = \theta_{\text{dyn}} + \beta$$

where:

$$\theta_{\text{dyn}} = \frac{1}{\pi}\int_0^t dt' \, \langle\psi(t)|H|\psi(t)\rangle$$

The non-adiabatic correction to the phase is related to the transition between eigenstates and can be described using the transition probability:

$$P_{m\to n} \sim \left|\frac{\langle u_n|\partial_t H|u_m\rangle}{E_n - E_m}\right|^2$$

In the case of a time $t >> \frac{1}{gap}$ meaning that the change to the Hamiltonian is really small compared to the overall Hamiltonian, and so that the eigenstate is evolving slowly over time (Adiabatic limit), we can express the dynamical phase and Berry phase such that :

- Dynamical phase is :

$$\frac{1}{\hbar}\int_0^t dt' E_n(K(t'))$$

- The Berry phase is :

$$\gamma_n = i\oint_C dk' \langle n(k)|\nabla_k|n(k')\rangle$$

We clearly see that time doesn't matter in the Berry phase expression so that only the trajectory is important. Another thing to notice is that we could also express it thanks to the Hamiltonian, which can be useful for numerical simulation computations.

Berry Phase and Connection

The Berry connection is defined as:

$$\mathcal{A}(\mathbf{k}) = i\langle u(\mathbf{k})|\nabla_{\mathbf{k}}|u(\mathbf{k})\rangle$$

where $|u(\mathbf{k})\rangle$ is the eigenstate of the Hamiltonian.
The Berry phase along a closed loop C in momentum space is:

$$\gamma = \oint_C \mathcal{A}(\mathbf{k}) \cdot d\mathbf{k}$$

If the loop encloses a Dirac point, the Berry phase is quantized:

$$\gamma = \pi$$

which is a signature of the topological nature of the system.

Berry Curvature and Berry Phase

The Berry phase is defined as:

$$\gamma = -\oint_C \mathcal{A} \cdot d\mathbf{k}, \tag{3.16}$$

where the Berry connection $\mathcal{A}$ is given by:

$$\mathcal{A} = i\langle u_n|\nabla_k|u_n\rangle. \tag{3.17}$$

The Berry curvature is then obtained as the curl of the Berry connection:

$$\Omega(k) = \nabla_k \times \mathcal{A}. \tag{3.18}$$

For a two-band system:

$$\Omega(\mathbf{k}) = i\sum_{m\neq n} \frac{\langle u_n|\partial_{k_x}H|u_m\rangle\langle u_m|\partial_{k_y}H|u_n\rangle - (x \leftrightarrow y)}{(E_n - E_m)^2}. \tag{3.19}$$

Applying this to the Dirac Hamiltonian, the Berry curvature takes the form:

$$\Omega(\mathbf{k}) = \pm\frac{1}{2}\frac{k_x^2 + k_y^2}{(k_x^2 + k_y^2)^{3/2}}, \tag{3.20}$$

which results in a quantized Chern number.

Geometric Interpretation

The Berry phase can be interpreted as the flux of the Berry curvature over a closed surface:

$$\gamma = \int_S \Omega(\mathbf{k}) dS. \tag{3.21}$$

Using Stokes' theorem:

$$\oint_C \mathcal{A} \cdot d\mathbf{k} = \int_S \Omega \cdot dS. \tag{3.22}$$

This indicates that the Berry curvature behaves like an effective magnetic field in parameter space.

Physical Consequences

- The presence of Berry curvature modifies the equation of motion for wave packets:

$$\dot{\mathbf{r}} = \nabla_k E - \dot{\mathbf{k}} \times \Omega(\mathbf{k}). \tag{3.23}$$

This leads to anomalous transport effects, such as the anomalous Hall effect.

- In the case of graphene, the Berry phase is π, which protects the Dirac points and prevents localization of carriers.

Simple example of a two-Level system

For a simple two-level system:

$$H = \frac{\Delta}{2}\sigma_z$$

the eigenstates are:

$$|+\rangle = \begin{pmatrix} \cos\frac{\theta}{2} \\ e^{i\phi}\sin\frac{\theta}{2} \end{pmatrix}, \quad |-\rangle = \begin{pmatrix} \sin\frac{\theta}{2} \\ -e^{i\phi}\cos\frac{\theta}{2} \end{pmatrix}$$

The Berry connection in this case is:

$$\mathcal{A} = \langle -|i\nabla_{\mathbf{k}}|-\rangle = \frac{1}{2}(1-\cos\theta)\nabla\phi$$

leading to a Berry curvature:

$$\Omega = \frac{1}{2}\sin\theta$$

Example: Berry curvature in graphene

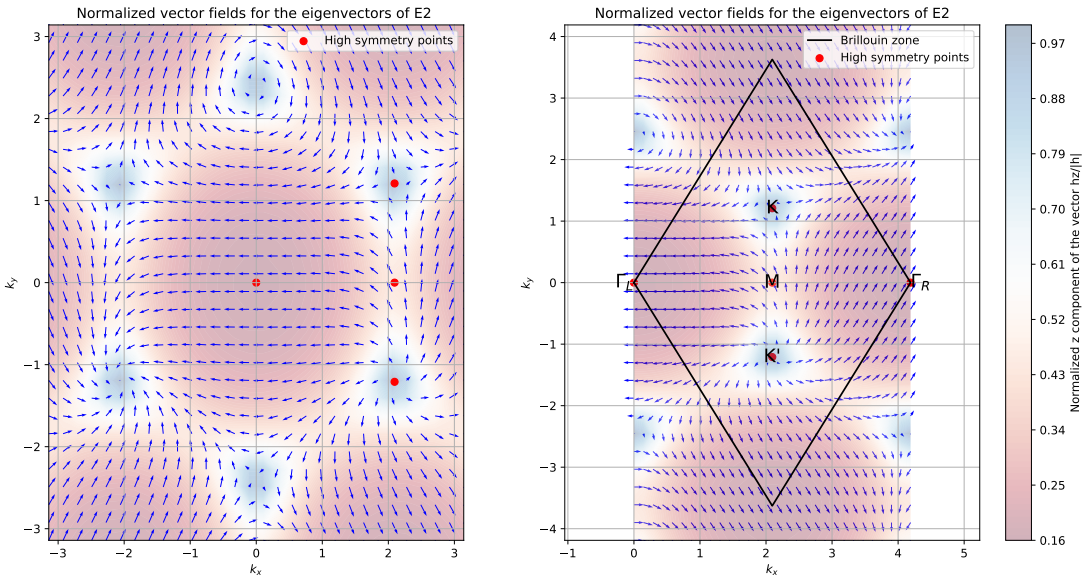

(a) (b)

Figure 3.19: Honeycomb lattice winding. At Dirac points, the z component of the eigenstates is stronger but K and Kp shows different winding.

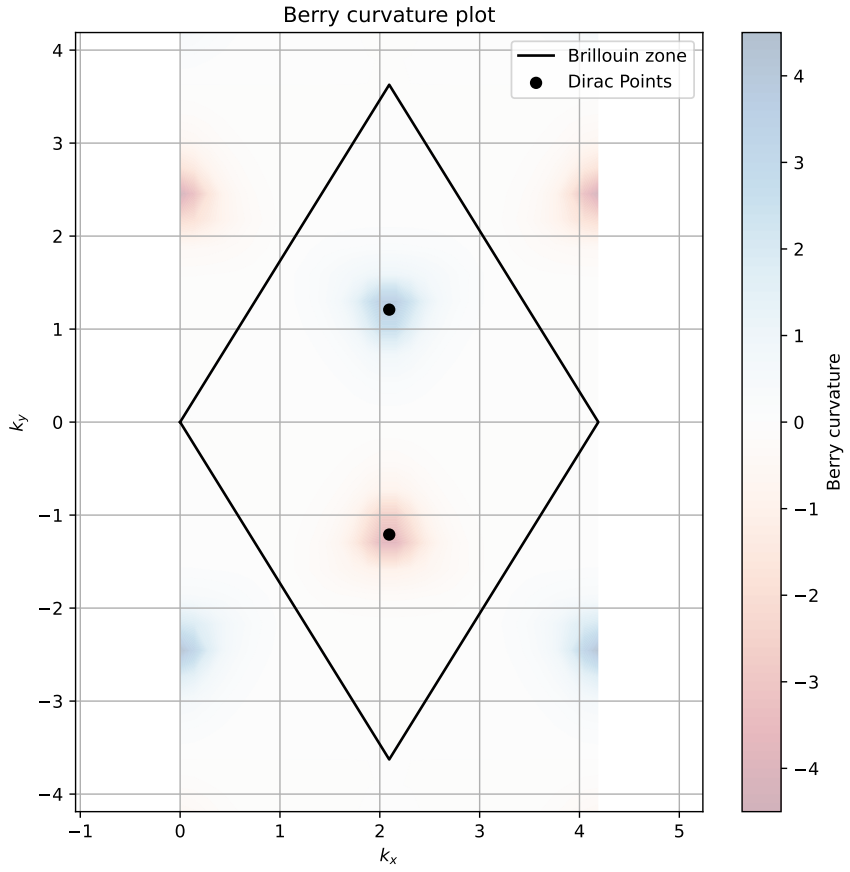

Figure 3.20: Berry curvature, we consider the diamond Brillouin zone in which we clearly see the Dirac points in the center

3.5 AB Phase in Haldane Model and Phase Diagram

In order to get an overall :

$$\int\int_{BZ} \Omega \neq 0$$

One needs to break time reversal symmetry $\mathcal{T}$. It means getting a different (and opposite) h_z for the two Dirac points of our Brillouin zone K_{DP} and $-K_{DP}$. It could be a $sin(k_y a)\sigma_z$ term. It is called **"topologically non trivial"**.

Rk: a magnetic field can brake time-reversal symmetry

The **Haldane model** proposes to connect the NNN (Next nearest neighboors) A-A and B-B sites of the honeycomb lattice thanks to tunneling terms $t_j^{A\prime}$ and $t_j^{A\prime}$

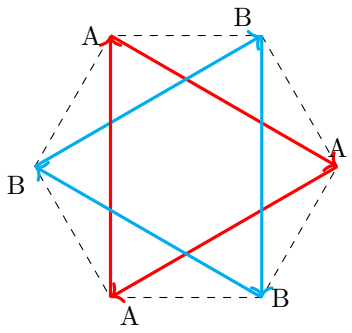

Figure 3.21: NNN tunneling between AA and BB sites

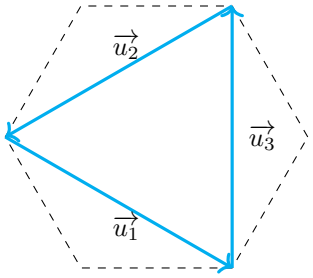

Figure 3.22: Defined vectors with right winding

Hamiltonian Components

On the diagonal:

$$h_i(\vec{k}) = \sum_j \left(\mathrm{Re}(t_j^{A\prime} + t_j^{B\prime}) \cos\left(\vec{k} \cdot \vec{v}_j\right) + \mathrm{Im}(t_j^{A\prime} - t_j^{B\prime}) \sin\left(\vec{k} \cdot \vec{v}_j\right) \right)$$

$$h_z(\vec{k}) = \sum_j \left(\mathrm{Re}(t_j^{A\prime} - t_j^{B\prime}) \cos\left(\vec{k} \cdot \vec{v}_j\right) + \mathrm{Im}(t_j^{A\prime} + t_j^{B\prime}) \sin\left(\vec{k} \cdot \vec{v}_j\right) \right) + \frac{\Delta}{2}$$

Simplified: same phase term to have a complex tunneling that is doing what we want (e.g., sin term).

let's note:

$$m = \mathrm{Im}(t_j^{A\prime} + t_j^{B\prime})$$

We do get such a distribution for the corresponding term:

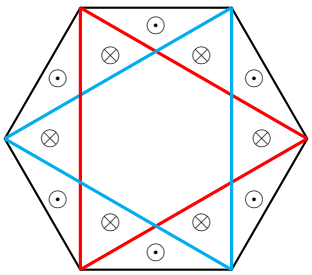

Figure 3.23: Haldane model flux distribution

Band Structure Evolution

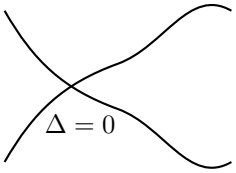

One Dirac point is not gapped so that in the limit cases, contributions sum and we do get a non-zero total geometric phase :

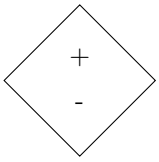

$(\int\int_{BZ} \Omega = 0)$

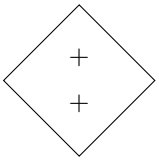

$(\int\int_{BZ} \Omega = 2\pi)$

$m = 0, \Delta > 0$ $\quad$ $\Delta = 0, m > 0$

Haldane's Phase Diagram

Conditions:

$$t_j^{A\prime} = t_j^{A\prime} \quad \text{for all } i, j$$

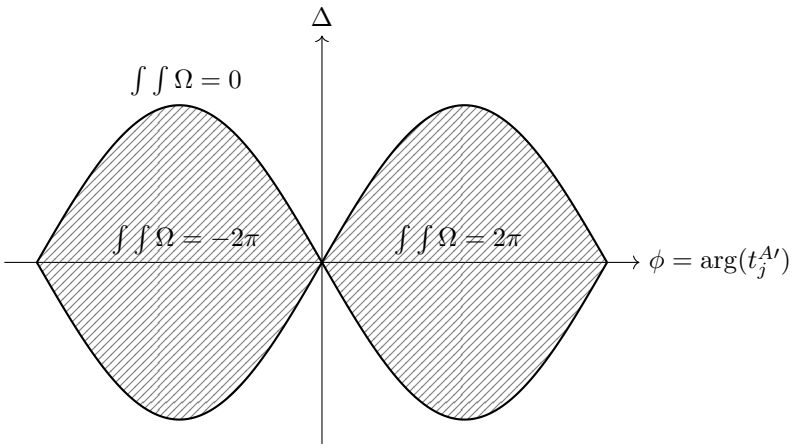

Figure 3.24: Haldane model phase diagram

The phase diagram above provides insights into the different regions of the system, depending on the phase ϕ and the parameter Δ. These regions are classified based on the topological properties of the system, as indicated by the integral of the Berry curvature, Ω. A natural progression from the discussion of this phase diagram is the concept of the **Chern number**, which plays a fundamental role in characterizing the topological nature of quantum systems.
The **Chern number** is a topological invariant that quantizes the Hall conductance in systems exhibiting topological phases. It is associated with the Berry curvature, Ω, and is given by the integral:

$$C = \frac{1}{2\pi} \int \int_{\text{BZ}} \Omega \, d^2k,$$

In the context of the Haldane model, the Chern number provides a way to classify the different phases of the system. For example, in regions where $\int \int \Omega = 2\pi$, the Chern number is $+1$, indicating a topologically nontrivial phase. On the other hand, when $\int \int \Omega = -2\pi$, the system exhibits a topologically trivial phase, with a Chern number of -1. The integral of the Berry curvature directly reflects the change in the system's topological properties across different regions of the phase diagram.

The Chern number thus acts as a robust classification tool for the different phases of matter, helping distinguish between systems with different topological characteristics. This concept is crucial not only in the study of the Haldane model but also in understanding other topological phenomena such as the quantum Hall effect.

The Quantized Hall Effect and its Relation to the Haldane Phase Diagram

The **Quantum Hall Effect (QHE)** occurs when a two-dimensional electron system is subjected to a strong perpendicular magnetic field at low temperatures. In this regime, the Hall resistance becomes quantized, and the system exhibits a discrete set of conductance plateaus, which are directly related to the **Chern number** of the system's wavefunctions. This phenomenon is deeply tied to the topological properties of the system, as described by the Berry curvature and the Chern number.

The Hall conductance in a system exhibiting the quantum Hall effect is quantized in integer multiples of a fundamental constant:

$$\sigma_{xy} = \frac{e^2}{h}\nu,$$

where ν is the filling function of the Landau levels in the system, and e and h are the charge of the electron and Planck's constant, respectively. This quantization arises due to the topological nature of the electron states in the system.

This can be derived from a simple model :

If we consider one cycle in the Brillouin zone, it does correspond to sideways movements by C sites so that :

$$h\dot{K} = F$$

$$K = K_0 + \frac{F \cdot t}{\hbar}$$

for t =T:

$$\frac{2\pi}{a} = \frac{F}{\hbar}T = eE\frac{2\pi}{h}$$

We do get $T = \frac{h}{Eea}$, and the current density for a 2D system is now written :

$$j_{2D_y} = n_{2D}v_y = n_{2D}\frac{ae}{T} = n_{2D}a^2E\frac{e^2}{h}$$

The filling function ν which determines the number of e^- per unit cell, can be defined such that:

$$j_{2D_y} = \nu\frac{e^2}{h}E$$

The Hall conductivity does now appear and "Quantum" in the quantum Hall effect comes from this filling.

To connect this to the **Haldane Phase Diagram**, recall that in the phase diagram, the integral of the Berry curvature Ω provides a measure of the topological charge of the system, and the value of this integral directly determines the Chern number.

As shown in the Haldane phase diagram, regions with $\int\int \Omega = 2\pi$ or $\int\int \Omega = -2\pi$ correspond to topologically nontrivial phases, where the Chern number is ± 1, while regions where $\int\int \Omega = 0$ correspond to topologically trivial phases, with a Chern number of 0. This directly links to the occurrence of the **Quantum Hall Effect**.

In these topologically nontrivial regions, the system exhibits **chiral edge states**, which are one-dimensional conducting states that exist at the boundaries of the system. These edge states are protected by the topology of the bulk system and are immune to disorder, which is why the Hall conductance remains quantized and robust against impurities.

In the diagram above, the regions where the Berry curvature integral equals 2π or -2π correspond to **topologically nontrivial phases**. In these phases, the **Chern number is ± 1**, indicating the presence of quantized Hall conductance and edge states. These edge states move in one direction along the boundary, which is a hallmark of the **Quantum Hall Effect**. Conversely, when the integral of the Berry curvature is zero, the system is in a **topologically trivial phase**, where the Hall conductance is zero, and no edge states exist.

The robustness of the quantum Hall effect comes from the fact that the Chern number is a **topological invariant**, meaning it is unaffected by small perturbations or impurities in the system. As a result, the system's conductance remains quantized even in the presence of disorder, as long as the topological phase is preserved.

Therefore, the phase diagram helps visualize the conditions under which the system exhibits the quantum Hall effect and the associated topological properties. It illustrates how the transition between different phases—driven by changes in parameters like ϕ and Δ—can result in a shift from a topologically trivial phase to a topologically nontrivial one, where the Hall conductance becomes quantized.

Example of interfaces

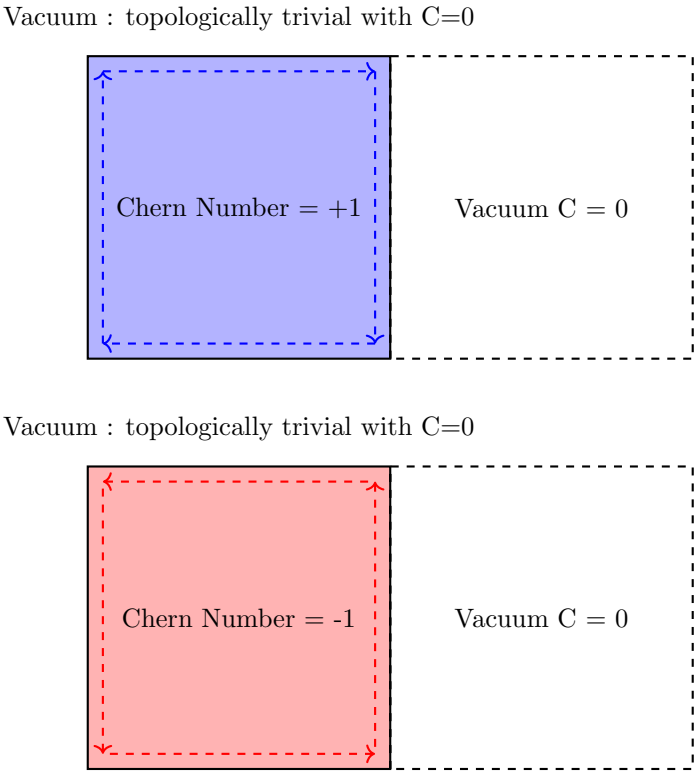

We can now talk more about an experimental point of view. We refer to "Transport" when talking about electrons travelling through these conductive channels. From the theory, those electrons should travel in an infinitesimal part at the edge of the sample. However, it is in reality non trivial.

Haldane situation

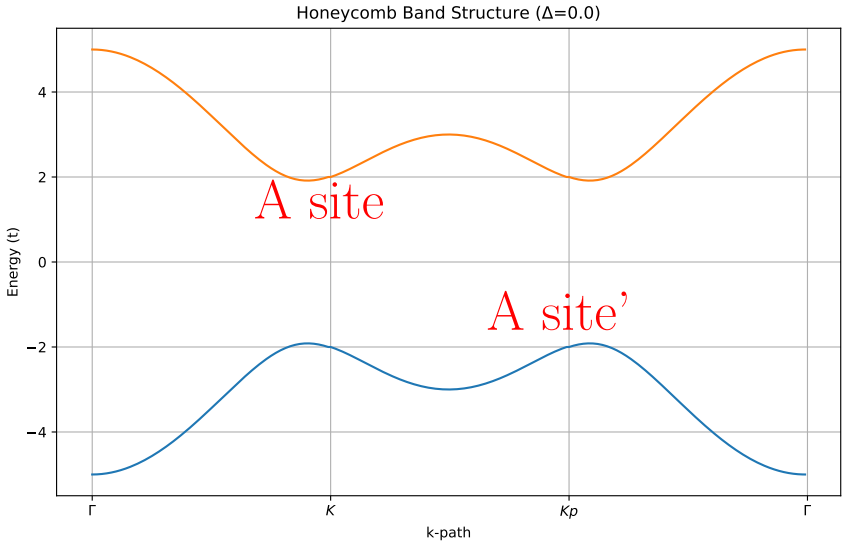

Figure 3.25: Band structure with broken symmetry

In that situation, we get state accross the gap: " the edge state is conductive" and has a direction.

Magnetic flux filling

Considering an atomic size unit cell, filling it with a magnetic field as strong as a magnetic flux seems completely unphysical in such a little area. Still, let's think about it because it is necessary to understand the quantized Hall effect.

With a translation symmetry every two sites:

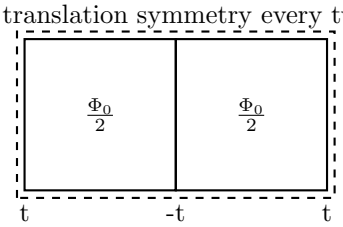

New unit cell

We do get one magnetic flux per "unit cell", and we can now create any other kind of unit cell respecting this condition.

With a translation symmetry every three sites:

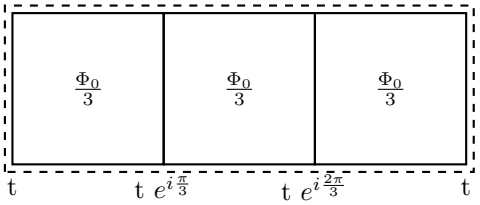

New unit cell

The unit cell is now three time larger than before and still contains Φ_0.

Now, what happens when we generalize this idea?

By varying the magnetic flux per plaquette, we can still define a unit cell as long as the total flux per unit cell is a rational multiple of the flux quantum, i.e., $\Phi = \frac{p}{q}\Phi_0$ where p and q are integers. This means that for every rational value of flux per plaquette, the system regains a form of periodicity—albeit with a larger unit cell.

This enlarged unit cell results in a band folding of the energy spectrum: the original band splits into q subbands. These bands can carry nontrivial topological information, such as Chern numbers, which determines quantized Hall conductance. Some bands are topologically nontrivial (Chern number $\neq 0$), while others are trivial (Chern number $= 0$).

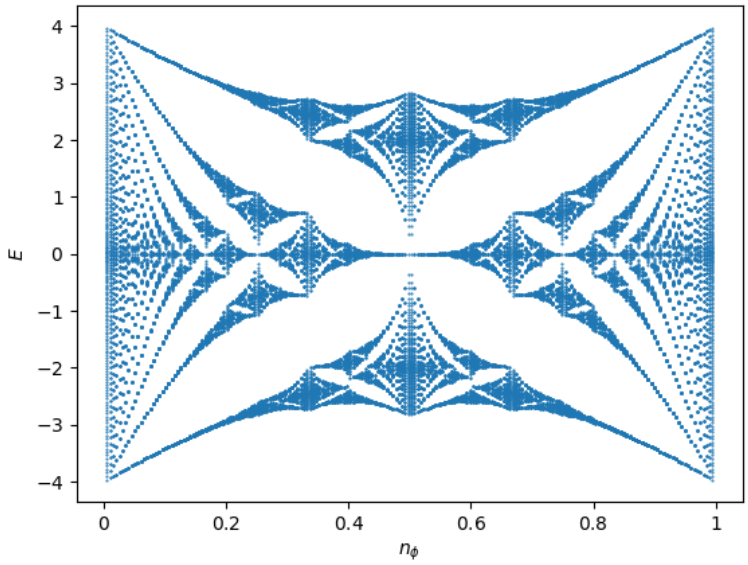

Figure 3.26: Hofstadter Butterfly. Landau levels distribution with respect to the flux filling.

When you plot the allowed energy levels of electrons in a 2D lattice as a function of the magnetic flux per plaquette Φ/Φ_0, you obtain a fractal structure known as the Hofstadter butterfly. This plot beautifully reveals how the energy spectrum splits and forms gaps at rational flux values. The intricate structure is not random—each gap can be labeled by a topological invariant, reflecting the quantized Hall response of the corresponding filled bands.

Key insight: The Hofstadter butterfly shows that the interplay between a periodic lattice potential and a uniform magnetic field leads to a highly nontrivial, self-similar energy spectrum. It's a striking example of how quantum mechanics, topology, and lattice geometry come together to produce emergent physical phenomena.

And what if spin matters?

Let's consider spin orbit coupling as an interaction such that :

$$h_\uparrow(K) \neq h_\downarrow(K)$$

It can be achieved in transition meta-dichalcogenides (TMDs). It can be MoS_2, $MoSe_2$, WS_2 or WSe_2. They are materials that we can get as monolayers and they have a direct bandgap with a hexagonal lattice.

In our honeycomb hamiltonian, we can add this term :

$$\Delta_\uparrow(K_{DP}) \neq \Delta_\downarrow(-K_{DP})$$

And this does lift the band structure depending on the spin orientation:

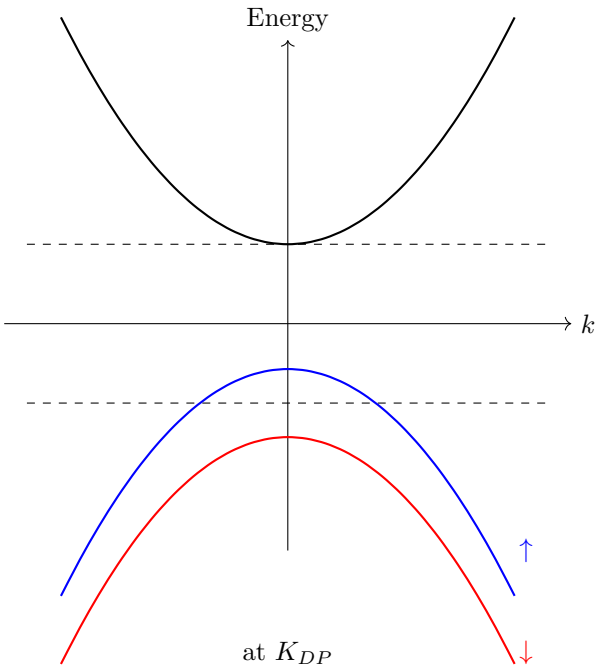

In the Kane-Mele model, we then get similar conductive edge states, but now Time-reversal symmetry is maintained : "Spin Hall effect".

Spin-Hall effect

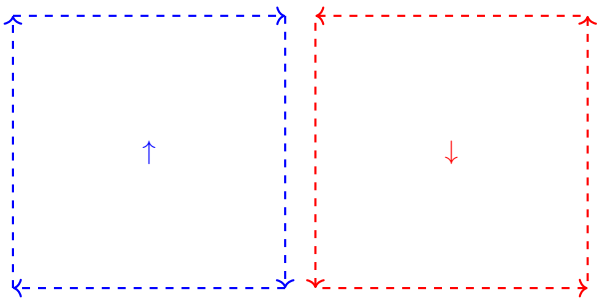

In 3D, it is also possible to get Dirac points called "Weyl points". One example is the TaAs. Other materials like Bi_2Se_3 are 3D TRS maintaining topologically insulated with an insulating bulk and Dirac metallicity on surface.

One of the most active research in this field concerns 2D stacks using different materials with matching lattices. The most famous example is hBN-Graphene (hexagnonal Boron Nitride on graphene, whom can tune the property of graphene). Moiré materials are part of those 2D stacks engineering and the aim is to modify the periodicity of a

lattice by using two layers on top of each others but with a twisting angle. The result is a big unit cell, meaning a little Brillouin zone and in such a unit cell, flux can be much bigger. If you are interested about this topic, you can read more litterature on twisted bilayer graphene and the magic angle which can give very flat bands.

3.6 Transport properties of Graphene

Transport Properties of Graphene

$$R = \frac{V}{I} = \rho\frac{l}{A}$$
$$I = \frac{V}{R} = \frac{w \cdot d}{\rho \cdot l} \cdot V = \frac{w \cdot d}{l} \cdot \sigma \cdot V = \frac{w \cdot d}{l} \cdot j$$
$$\sigma = \frac{1}{\rho}, \quad j = \sigma E$$

Ohm's Law:

$$j = \sigma E$$

Carrier density:

$$\sigma = \frac{ne^2\tau}{m} \Rightarrow \mu = \frac{e\tau}{m} \quad \text{(mobility)}$$

Assumptions:

- Electrons are treated as particles with an effective mass m^*.
- Classical model.
- Doesn't apply in any material like graphene!

Measurement Techniques and Setup

1. **Two-points measurement:**

$$V = IR \Rightarrow R = \rho\frac{l}{A}$$

2. **Four-points measurement:**

$$V = IR_{\text{sample}}, \quad \text{(eliminates contact resistance)}$$

The four-point probe technique is used to measure the **intrinsic resistance** of a sample, eliminating contributions from contact and lead resistances.

Working Principle

- Current is injected using two **outer contacts** (I_+ and I_-).
- Voltage is measured across two **inner contacts** (V_+ and V_-).
- The voltmeter draws negligible current, so the voltage drop only reflects the resistance between V_+ and V_-.

$$R_{\text{sample}} = \frac{V_+ - V_-}{I}$$

Diagram

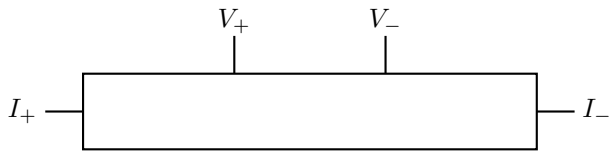

Hall Bar Geometry

The Hall bar geometry is used for measuring both **longitudinal** and **transverse (Hall)** resistances. It is widely used in characterizing 2D materials such as graphene.

Features:

- Enables measurement of longitudinal resistance R_{xx} and Hall resistance R_{xy}.
- Useful for extracting carrier density, mobility, and observing quantum Hall effects.
- Often combined with a backgate to control carrier concentration.

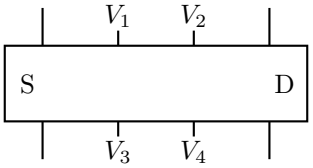

Substrate and Material Example

Substrate: SiO_2 (285 nm) on highly doped Si (backgate)
Dielectric: SiO_2

Graphene Properties:

- High mobility: $\mu \sim 10^5\,\mathrm{cm}^2/\mathrm{Vs}$
- Ballistic transport regime possible
- Acts as a 2D Dirac fermion system

Gate Control:

$$V_g \Rightarrow \text{controls charge carrier density}$$

Density of States (DOS):

$$\text{Linear in graphene:} \quad \rho(E) \propto |E|$$

Chapter 4

Interacing electrons

Until now, we considered electrons as independent particles but they actually interact strongly between them. Understanding those interactions will bring us towards understanding superconductivity and other phenomomena.

4.1 Hubbard model

4.1.1 Bosons and Fermions

First things first, let's briefly recall some knowledges about operators and formalism.

Let's consider this two particles wafunction :

$$|\Psi\rangle = b_{x,y}|p_{1x}\rangle \times |p_{2y}\rangle$$

Where "p_{1x}" means particle 1 in state x.

The exchange operator is defined such that

$$\hat{P}|\Psi\rangle = b_{y,x}|p_{1y}\rangle \times |p_{2x}\rangle = \pm|\Psi\rangle$$

And applying two times the operator : $\hat{P}(\hat{P}(|\Psi\rangle)) = |\Psi\rangle$, meaning $b_{x,y}^2 = 1$. Bosons are defined for the "+" case when Fermions are the "-" case.
Consequence: A state can not be occupied with more than one fermion in any basis.

4.1.2 Commutator

The **anti-commutator** of two operators is defined as:

$$\{A, B\} = AB + BA$$

Now, consider the **fermionic creation** and **annihilation** operators, $c_x^\dagger$ and c_x. They obey the following key algebraic relations:

- **Nilpotency (no double occupancy on the same site):**

$$c_x^\dagger c_x^\dagger \, |\text{any state}\rangle = 0$$

$$\Rightarrow \{c_x^\dagger, c_x^\dagger\} = 0$$

$$\{c_x, c_x\} = 0$$

This means that applying the creation (or annihilation) operator twice on the same site gives zero. You cannot create (or destroy) two identical fermions at the same location. This is a direct algebraic consequence of the **Pauli exclusion principle**, which states that no two fermions can occupy the same quantum state.

- **Canonical anti-commutation relation:**

$$\{c_x, c_y^\dagger\} = \delta_{x,y}$$

This reflects the orthonormality of single-particle states, assuming $\langle x|y|x|y\rangle = \delta_{x,y}$. It ensures that creating a particle at site y and annihilating one at site x yields a nonzero result only when $x = y$.

Conclusion: These algebraic rules encode the *Pauli exclusion principle* in operator form. The occupation number per site is restricted to either 0 or 1, consistent with the fermionic nature of particles like electrons.

Let's write $n_x = c_x^\dagger c_x$ ($\langle 1|n_x|1\rangle = 1$ and $\langle 0|n_x|0\rangle = 0$).

4.1.3 Two sites and one electron with possible tunneling

We can consider this simple case with one only one electron $|\uparrow\rangle$ which can tunnel between two sites.

The Hamiltonian is :

$$\hat{H} = -t(c_1^\dagger c_2 + c_2^\dagger c_1)$$

The basis is :

$$\{|\uparrow, 0\rangle; |0, \uparrow\rangle\}$$

Computing the different component of the Hamiltonian like :

$$H_{11} = \langle\uparrow, 0|\hat{H}|\uparrow, 0\rangle = -t\langle 0, 0|c_{1\uparrow}(c_1^\dagger c_2 + c_2^\dagger c_1)c_{1\uparrow}^\dagger|0, 0\rangle = 0 + 0 = 0$$

We finally get :

$$H = \begin{bmatrix} 0 & -t \\ -t & 0 \end{bmatrix}$$

4.1.4 Several electrons and interactions

What interactions should we consider? To answer this question let's remind that the distribution of electrons is really localized on the site they're affected to. This means we can start by taking into account the interactions between e^- on the same sites. Many interactions can be added but let's be simplistic for now.

The parameter U is defined such that :

$$H_{U,i} = Un_{i\uparrow}n_{i\downarrow} = Uc_{i\uparrow}^\dagger c_{i\uparrow}c_{i\downarrow}^\dagger c_{i\downarrow}$$

It is the resulting energy penalty due to double occupancy on a site. The total Hamiltonian result in:

$$H_{TOT} = \sum_{\langle i,j\rangle,\sigma} (-t_{ij}c_{i\sigma}^\dagger c_{i\sigma} + h.c) + \sum_{i,\sigma} \epsilon_{i,\sigma}n_{i,\sigma} + \sum_i Un_{i\uparrow}n_{i\downarrow}$$

The interesting case is the when we have two electrons and two sites. With such interactions, if we choose both electrons having the same spins $\uparrow$ for example, then we obtain a trivial basis $|\uparrow, \uparrow\rangle$ and E=0.

We need to start from the case with one electron up and one electron down :

$$Basis = \{|\uparrow,\downarrow\rangle; |\downarrow,\uparrow\rangle; |D,0\rangle; |0,D\rangle\}$$

D means double occupancy up and down.

Every of these eigenstates is obtained from $|0,0\rangle$ applying the wright operators : $c^\dagger_{1\uparrow}c^\dagger_{2\downarrow}|0,0\rangle = |\uparrow,\downarrow\rangle$. Depending on the choice of the placement of the operators in the Hamiltonian, there will be a minus sign for the $|\uparrow,\downarrow\rangle$.

Computing the Hamiltonian of the system we do get:

$$H = \begin{bmatrix} 0 & 0 & -t & -t \\ 0 & 0 & \mp t & \mp t \\ -t & \mp t & U & 0 \\ -t & \mp t & 0 & U \end{bmatrix}$$

In the upper left square of this matrix there is no components meaning no flip-flop terms which would correspond to direct magnetism. This magnetism is however still possible through different transformations with this Hamiltonian.

The Energy of the eigenstate $\widetilde{S}$ is :

$$E_{\widetilde{S}} = \frac{\sqrt{16t^2+U^2}-U}{2}$$

The eigenstate $\widetilde{S}$ has a shape:

$$|\widetilde{S}\rangle \propto (\sqrt{16t^2+U^2}-U)(|\uparrow,\downarrow\rangle - |\downarrow,\uparrow\rangle) + 4t(|D,0\rangle + |0,D\rangle)$$

In the limit where U>>t : $E_{\widetilde{S}} = \frac{-4t^2}{U}$. It is the **Heisenberg limit** which leads to antiferromagnetic type of sites that are energetically more favorable. More generally, a small value of U tends to favor double occupancy.

4.1.5 Hubbard Model Atomic Limit ($t/U \to 0$)

Key Characteristics:

- **Localized Electrons:** Kinetic energy (hopping t) is negligible compared to on-site Coulomb repulsion (U). Electrons are strongly localized.
- **No Band Formation:** Energy levels are determined by local potential and U, not electron delocalization.
- **Atomic-like Energy Levels:** Sites can be empty (0 e^-), singly occupied (1 e^-), or doubly occupied (2 e^- with energy cost U).
- **High Degeneracy:** Multiple degenerate ground states possible for a given electron number and lattice size.
- **Mott Insulator Behavior (Half-filling):** A gap of $\sim U$ opens between lower and upper Hubbard bands, leading to insulating behavior.

Theoretical Significance:

- **Starting Point for Strong Coupling Theories:** Perturbation theory around the $U \to \infty$ limit.
- **Understanding Local Correlations:** Isolates the effects of on-site electron-electron interactions.

- **Benchmarking for Numerical Methods:** Exact solutions can be used to test numerical approaches.
- **Qualitative Insights:** Provides basic understanding of Mott transitions and strong correlation effects.

Applications and Extensions:

- Understanding Mott insulators.
- High-temperature limit in some cases.
- Extension to more complex Hubbard models.
- Foundation for Dynamical Mean-Field Theory (DMFT).

In Summary: The atomic limit is a crucial simplification of the Hubbard model ($t \ll U$) that highlights the dominant role of local Coulomb interactions and provides a foundation for understanding strongly correlated electron systems and the Mott insulating state.

4.1.6 SU(2) Symmetry

To better understand the structure of spin states and their interactions in the Hubbard model, it's important to recognize the underlying **SU(2) symmetry**.

Definition: SU(2) is the group of unitary 2×2 matrices with determinant 1. It governs spin rotations in quantum mechanics. In the context of the Hubbard model, SU(2) symmetry reflects the invariance of the system under global spin rotations.

Spin Operators: Define the total spin operators as:

$$\vec{S}_i = \frac{1}{2} \sum_{\alpha,\beta} c_{i\alpha}^\dagger \vec{\sigma}_{\alpha\beta} c_{i\beta}$$

where $\vec{\sigma} = (\sigma^x, \sigma^y, \sigma^z)$ are the Pauli matrices. These operators satisfy the standard spin algebra:

$$[S_i^a, S_j^b] = i\delta_{ij}\varepsilon^{abc} S_i^c$$

Conservation Laws: The SU(2) symmetry implies that the total spin

$$\vec{S}_{\text{tot}} = \sum_i \vec{S}_i$$

commutes with the Hubbard Hamiltonian:

$$[H, \vec{S}_{\text{tot}}] = 0$$

This means that the total spin and its projection S_{tot}^z are conserved quantities. As a result, the eigenstates of the Hamiltonian can be classified by total spin S and magnetic quantum number m_S.

Singlet and Triplet Classification: SU(2) symmetry naturally leads to the classification of two-electron states into:

- **Singlet (S = 0):** antisymmetric in spin, symmetric in space

$$|S\rangle = \frac{1}{\sqrt{2}}(|\uparrow,\downarrow\rangle - |\downarrow,\uparrow\rangle)$$

- **Triplet (S = 1):** symmetric in spin, antisymmetric in space

$$\begin{aligned} |t_1\rangle &= |\uparrow,\uparrow\rangle \\ |t_0\rangle &= \frac{1}{\sqrt{2}}(|\uparrow,\downarrow\rangle + |\downarrow,\uparrow\rangle) \\ |t_{-1}\rangle &= |\downarrow,\downarrow\rangle \end{aligned}$$

4.1.7 Singlet, triplet states and entanglement

Let's look at the Energy plot over U normalizing by the tunneling:

Ground State Energy $E_{\widetilde{S}}/t$ vs. U/t

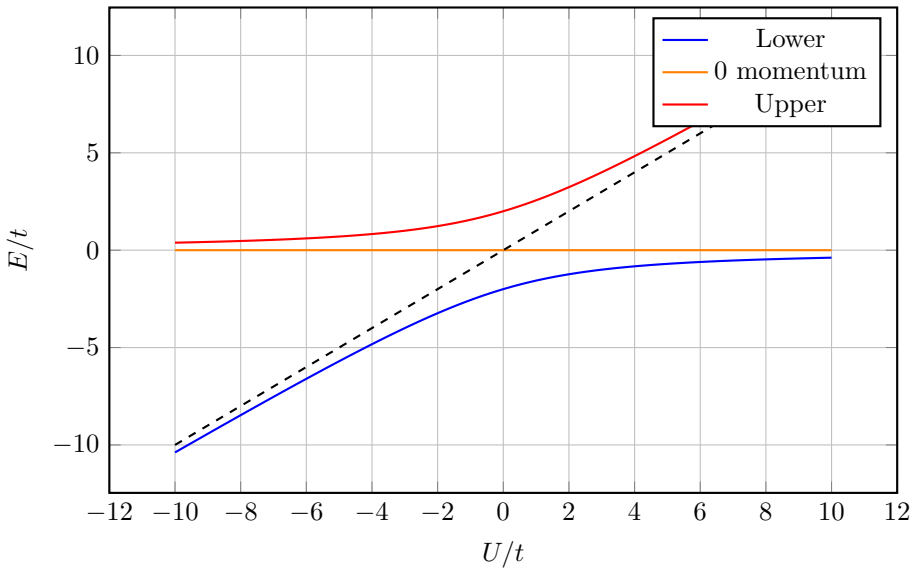

Few interesting things appear here, and let's focus in the $t \ll U$ limit. First, let's try to understand the 0 momentum state (orange). We do have a **triplet state** with 0 energy as those three states are degenerate and sums up to 0 in the case of 2 electrons :

- $t_1 = |\uparrow,\uparrow\rangle$
- $t_{-1} = |\downarrow,\downarrow\rangle$
- $t_0 = \frac{1}{\sqrt{(2)}}(|\uparrow,\downarrow\rangle + |\downarrow,\uparrow\rangle$

It is equivalent to an overall spin number S=1 with three possible projections :

- $t_1 = |S = 1, m_S = 1\rangle$
- $t_{-1} = |S = -1, m_S = -1\rangle$
- $t_0 = |S = 0, m_S = 0\rangle$

Applying a magnetic field would break symmetry and those projections would split in energy. The SU(2) symmetry guarantees degeneracy of the triplet states in the absence of a magnetic field but the singlet–triplet splitting observed in the energy spectrum is purely due to interactions (like the Hubbard U and hopping t), not symmetry breaking.

The lower and upper curves correspond to an eigenstate :

$$|\widetilde{S}\rangle \propto (|\uparrow,\downarrow\rangle - |\downarrow,\uparrow\rangle) + (|D,0\rangle + |0,D\rangle)$$

In the ground state case :

$$|S\rangle \propto |\uparrow,\downarrow\rangle - |\downarrow,\uparrow\rangle$$

which does merge with the Heisenberg limit, and its energy is $E_S = -\frac{4t^2}{U}$. This state is a singlet state equivalent to $|S = 0, m_S = 0\rangle$. In this simple basis, if you do measure the first spin Up, you know that the spin on site 2 have to be Down. It is called a **Bell state** and is referred as "Entanglement".

The upper band in this limit corresponds to the double occupancy term which is way higher in energy.

Quick remark for triplet state in NV centers

As you may recall, NV centers have a triplet state with a zero field splitting of 2.87 GHz between states $|m_S = \pm 1\rangle$ and $|m_S = 0\rangle$. This splitting exists because there is a broken symmetry here that Hubbard Hamiltonian did not break, which is the SU_2 symmetry.

4.1.8 Two unconnected pairs of sites

Let's now consider a system of four sites consisting of two unconnected pairs. Let's call the pairs A and B. The constructed wavelength can be written :

$$|\Psi\rangle = \Delta_A^+ \Delta_B^+ |0\rangle = \Delta_B^+ \Delta_A^+ |0\rangle$$

with :

$$\Delta_A^+ = c_{1\uparrow}^+ c_{2\downarrow}^+ - c_{2\uparrow}^+ c_{1\downarrow}^+$$

and same for B sites. It is symmetric under exchange of 2 singlets, which is equivalent to say that a singlet looks like a Boson. Indeed, thise are called "**composite Bosons**", and it means they can Bose-Enstein condensate evenif the underlying nature is fermions!

4.1.9 Valence bond solid

In the square lattice limit, we can get long range order, meaning that we know with a high probability what spin states we have at any point if we do know the state on one site: it is an antiferromagnet configuration. It is also reffered as spontaneous symmetry breaking.

However, there are very different macroscopic ground states which are in theory equivalent (a superposition), but in reality, an impurity somewhere or a residual magnetic field would result in an non trivial state because the system is so sensitive to external interactions. It also happening when measuring in cold atoms system, it does break this superposition state.

A transition between AFM and VSB phasis can be observed in materials like $TlCuCl_3$ by applying pressure. here is a schematic drawing about the phase diagram:

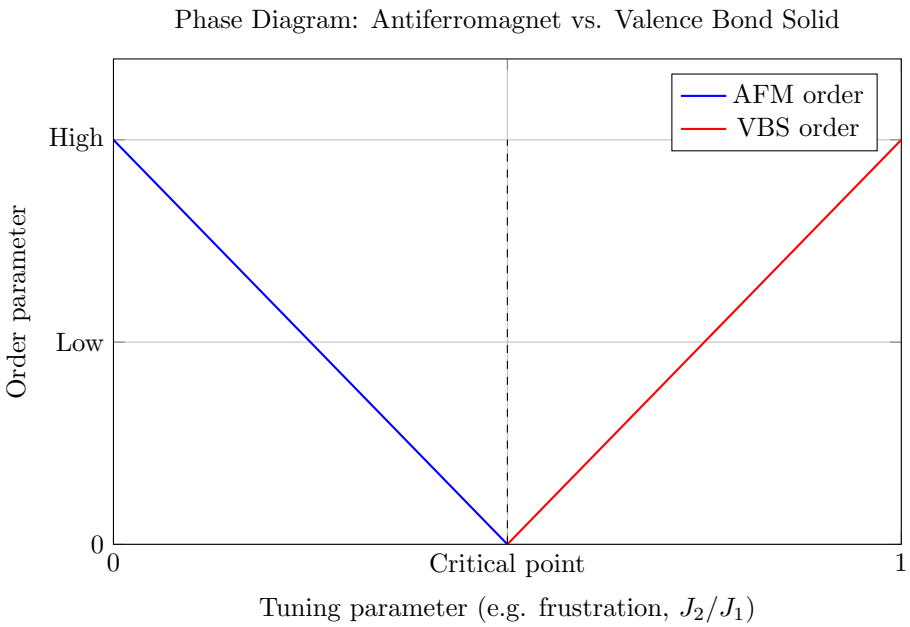

Frustration is a concept referring about the possible choice for organization of the spins when you have some well defined symmetries like triangles. Let's take the triangle as an example of a system with SU(2) symmetry in which we can still choose the spin distribution:

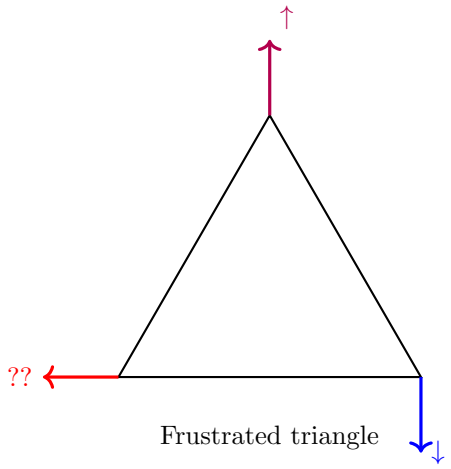

Two possible choices can de made:

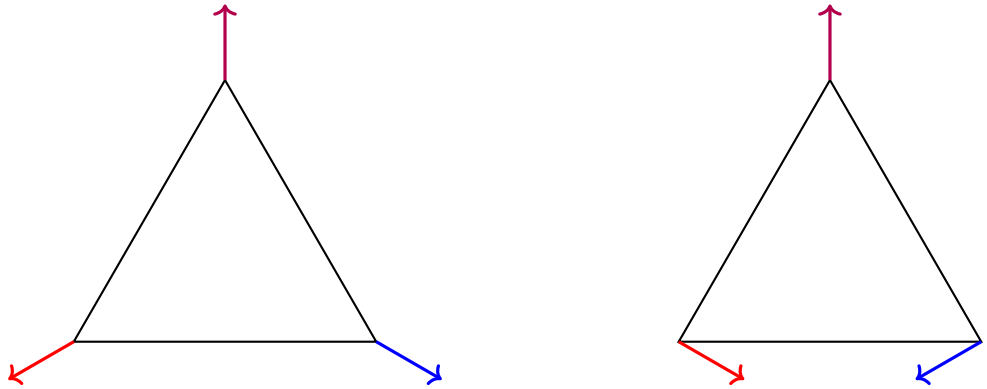

By extending this to a lattice, the system have a "little" frustration because it has a bit of hard time ordering. In some more complicated geometries, it can result in an important frustration like for example the crystal structure of herbertsmithite.

4.2 Superconductivity Phenomenology

In 1911 happened the discovery of superconductors by Onnes, made possible after great improvements on cryogenic liquids. Researchers wanted to answer the question :

How the resistivity of a material scale with temperature?

The first material successfully tested at low temperature thanks to liquid helium was Mercury (Hg), because it was the most refinable metal at that time. Close to room temperature, the current voltage formula is well known as Ohm's low, but superconductors show a breakdown of resistance at a given "critical temperature" where R=0.

Ohm's Law as we know it

$$U = RI$$

Also written :

$$\vec{J} = \sigma \vec{E}$$

What does that mean? it means a force that's proportionnal to a velocity, which is not the classical scheme derivated from Newton's equation. However, it has to be understand as a friction, a resistance as we increase the current. Carriers move and reach a steady-state with a scattering term that we can explain with a classical approach in the Drude model becuase Ohm's law does breakdown in some limits like at low temperature.

4.2.1 Drude Model (Classical Theory)

Electrons accelerate under the influence of an electric field, but experience scattering:

$$\frac{\mathrm{d}\vec{p}}{\mathrm{d}t} = -e\vec{E} - \frac{\vec{p}}{\tau}$$

Where τ is the scattering time. charge density wise, it is also written :

$$\frac{\mathrm{d}\vec{j}}{\mathrm{d}t} = \frac{nq^2}{m}\vec{E} - \frac{\vec{j}}{\tau}$$

Here, m is the effective mass of the moving charge and n is the charge density.

In the steady state :

$$\vec{j} = \frac{ne^2\tau}{m}\vec{E}$$

We note :

$$\sigma_0 = \frac{ne^2\tau}{m}$$

and define the conductivity as :

$$j = Re\{\sigma E\}$$

Limiting behavior: As $T \to 0$, $\tau \to \infty \Rightarrow \sigma \to \infty$ Meaning that charges would move without any scattering and :

$$\frac{\mathrm{d}\vec{j}}{\mathrm{d}t} = \frac{nq^2}{m}\vec{E}$$

If we have a AC electric field $\propto E_0 sin(\omega t)$:

$$j \propto \int E(t) \propto \frac{1}{\omega} cos(\omega t)$$

This correspond to a 90° shifted current density with respect to the Electric field, and also a time dependency. This phase shift is directly introduced by the resulting imaginary conductivity $\sigma_S = \frac{ine^2}{m\omega}$.

Let's try to understand intuitively what's happening with this simple model for a superconductor.

General solution

The general solution of the conductivity is :

$$\sigma_D = \frac{nq^2\tau}{m(1 - i\omega\tau)}$$

In most metals $\tau \approx 10^{-15}s$ so a frequency close to 10 THz. Trying to do what is called "THz spectroscopy" is a way to proceed conductivity measurement in materials like superconductors.

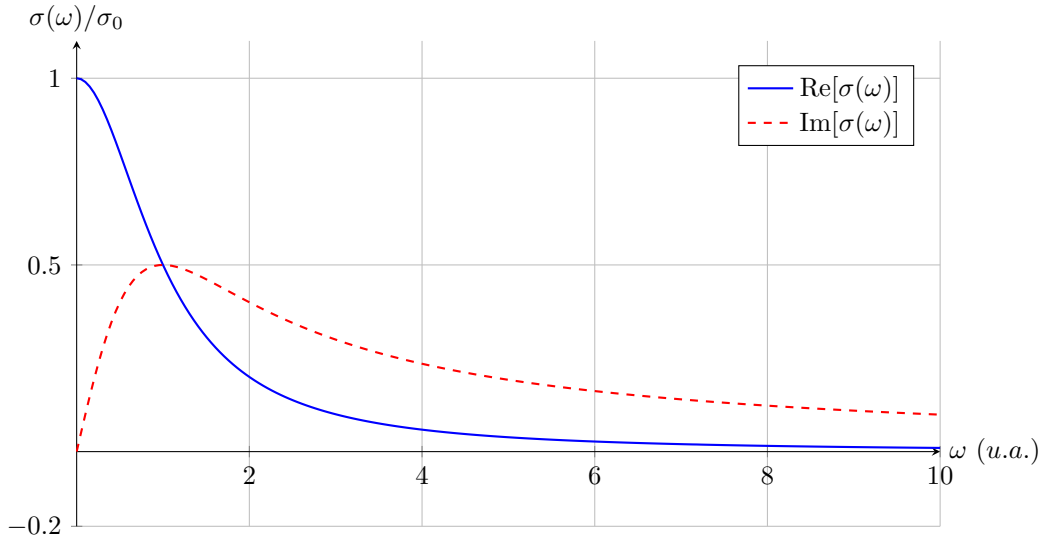

In the limit $\tau \to \infty$ we do get a different behavior :

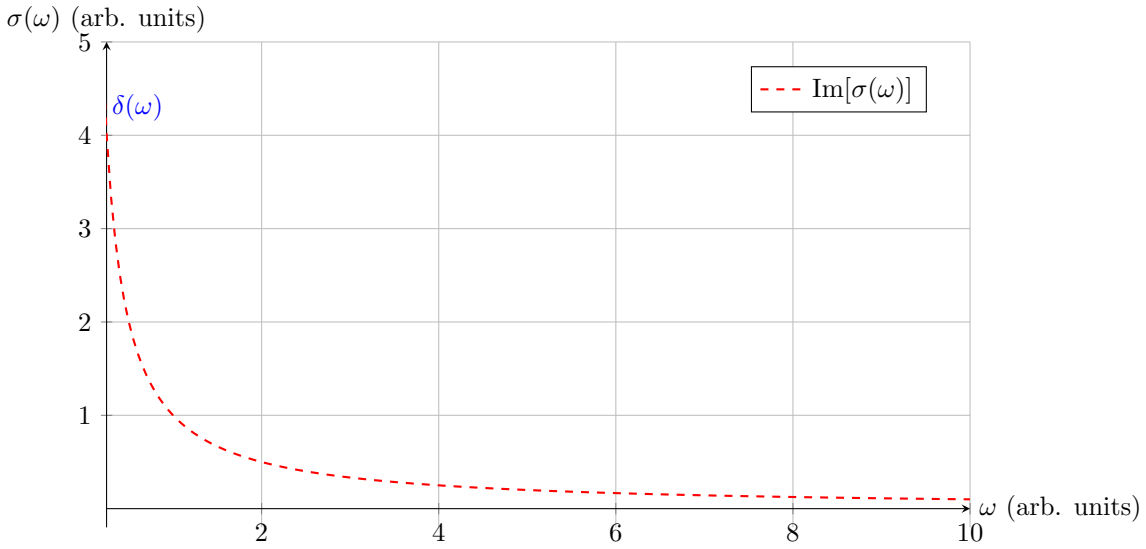

This last case correspond to a superconductor with a step of the real part of the conductivity at $\omega = 2\Delta$. This gap is called "Optical gap". We clearly see the imaginary part diverging as $\frac{1}{\omega}$ meaning SC conductance is infinite only at infinitely low frequencies.

Thinking in terms of equivalent electric scheme, we can model it like:

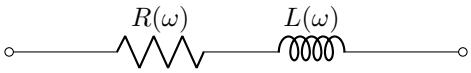

L(ω) is the kinetic inductance.

The conductivity in this case indeed scale as $\frac{1}{\omega}$, and that does correspond to the following equation :

$$\frac{\mathrm{d}\vec{j}}{\mathrm{d}t} = \frac{n_S q^2}{m}\vec{E}$$

This equation is known as the **1st London equation**. n_S is referring to an "empirical density" that was not so clear for superconductors at first.

Then, we can summarize that superconductors are better conductors only in the DC limit, because that won't be true anymore if the frequency increases too much.

If we want to measure the V-I behavior of a superconductor, we can use a simple voltage source and a resistor to flow a current. Meaning that it is the steady state of the electronic circuit that imposes the current. Doing such an experiment reveals the critical current value as shown on this curve:

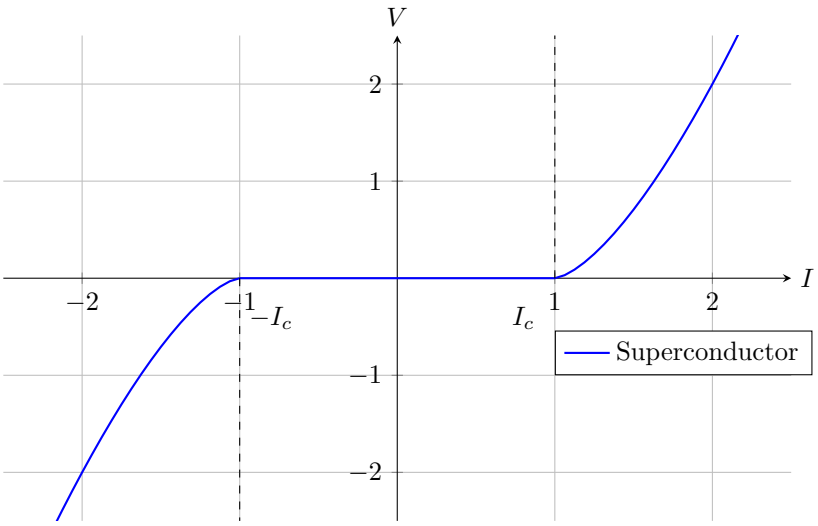

How to understand that we can have $R = 0$ but no infinite I_C then ?

Superconductors conductivity at finite temperature (meaning below $T_C/2$) can be expressed as :

$$\sigma = \sigma_D(n_n) + \sigma(n_s)$$

n_s are the superconducting electrons and increasing too much the current will force the normal electrons (n_n) to move and we can get a bit of dissipation in this regime.

4.2.2 Properties of SC in a magnetic field

An unexpected consequence of superconductivity was also discovered: magnetic-field permeability. That is to say, a superconductor is able to expel a magnetic field when entering the SC state. Eddy currents were already known and expected at this time because observed in copper for instance, but magnetic field permeability was not.

Let's try to understand through the maths what would happened wit a magnetic field.

Superconductor in a B field

let's first think about a cylindrical SC with longitudinal $\vec{B}$:

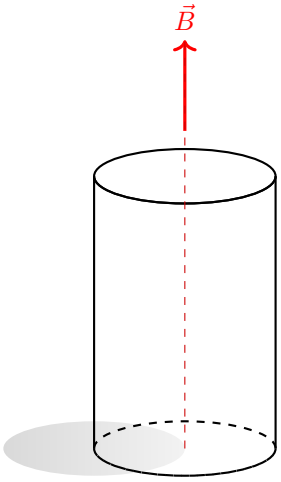

Cylinder

Faraday's law of induction gives:

$$\nabla \times \vec{E} = -\frac{\partial \vec{B}}{\partial t}$$

Adding the 1st London equation we do get the following equation:

$$\vec{E} = \frac{\partial \vec{J}}{\partial t} \cdot \frac{m}{n_s e^2} \Rightarrow \frac{m}{n_s e^2} \nabla \times \frac{\partial \vec{J}}{\partial t} = \partial_t \vec{B}$$

This equation represents the Eddy currents in a perfect conductor in response to an applied magnetic field.

Let's now add Ampère's law to this:

$$\nabla \times \vec{B} = \mu_0 \vec{J} \Rightarrow \vec{J} = \frac{1}{\mu_0} \nabla \times \vec{B}$$

From operators equivalence and Gauss's law we do get that:

$$\nabla \times \nabla \times \vec{B} = \nabla(\nabla \cdot \vec{B}) - \nabla^2 \vec{B} = -\nabla^2 \vec{B} \quad \text{since} \quad \nabla \cdot \vec{B} = 0$$

Now combining the previous results:

$$\partial_t (-\frac{1}{\mu_0} \nabla^2 \vec{B} + \frac{m}{n_s e^2} \vec{B}) = 0$$

The solutions of this equation are the possible fields in a perfect conductor. A typical length parameter can be defined like:

$$\lambda_L^2 = \frac{m}{\mu_0 n_s e^2}$$

It is the **London penetration depth**, which meaning is how long a magnetic field penetrates in a SC. More importantly, it scales with $\frac{1}{\sqrt{n_s}}$, with electrons that are turning due the external magnetic field that can expel a given amount of $\vec{B}$.

One possible solution for this equation is a constant field over time.

In the 30^s, Meissner observed an expulsion of magnetic field when crossing the SC phase transition. The idea of the London brothers was to say that the all-part in parentheses could be 0:

$$-\nabla^2 \vec{B} + \frac{1}{\lambda_L^2}\vec{B} = 0$$

This equation is easy to solve and called the **2nd London equation**.

Restricting to a 1D problem :

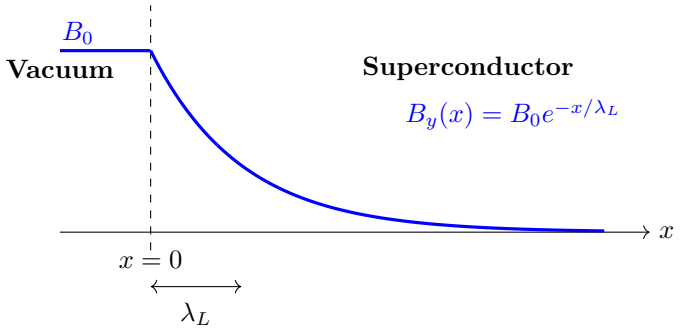

λ_L is typically small in cold superconductors : 10-100 nm. However, this value can get very large. Measuring this length is a way to measure n_S nowadays. You can measure the magnetic field with films sensitive to polarization rotation of light.

This behavior is different from a perfect diamagnet because we would get :

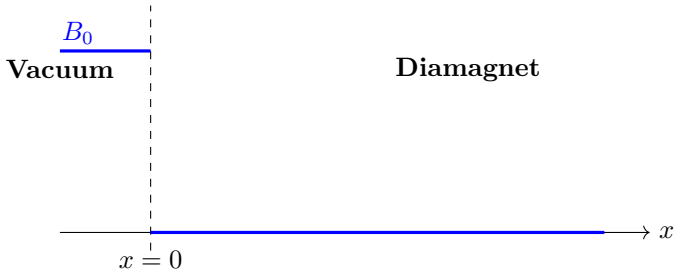

Field or zero field cooling

Let's consider a superconductor and a perfect conductor. Two paths are possible to be in a given state of temperature and external magnetic field. The first one consist in cooling down the phase transition before applying a magnetic field, it is the zero field cooling. The later is cooling down with the external field applied:

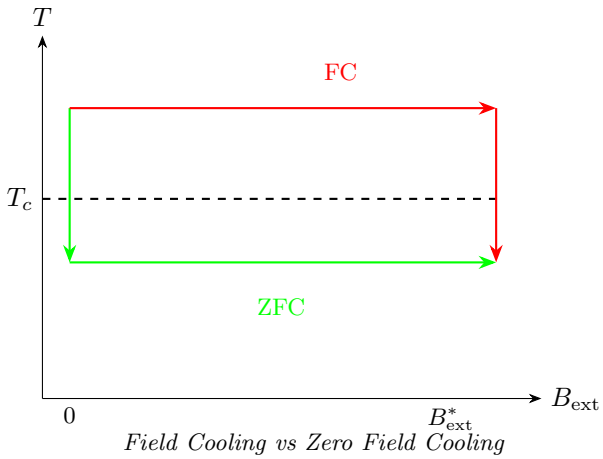

Field Cooling vs Zero Field Cooling

The perfect conductors and superconductors will behave the same in the Zero field cooling, expelling any applied magnetic field. It means that the superconductor will actively expel a magnetic field reorganizing its current to create a perfect diamagnet. It is the classic **Meissner effect**.

The interesting case is the field cooling, in which, at first a magnetic field would enter the superconductor :

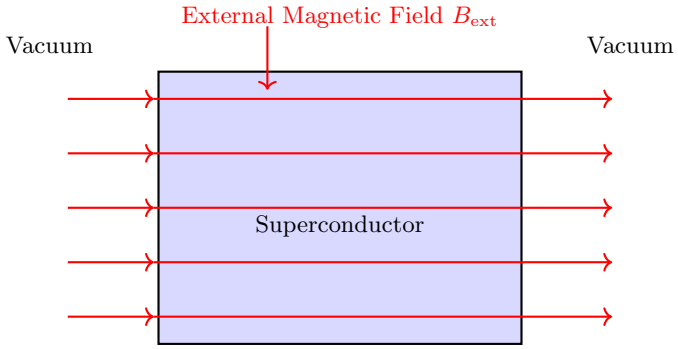

Then, when reaching Tc, the superconductor would ideally exclude the field as it becomes superconductive but in reality because of finite cooling rates, imperfections or chosen geometry, magnetic flux can be trapped inside the material

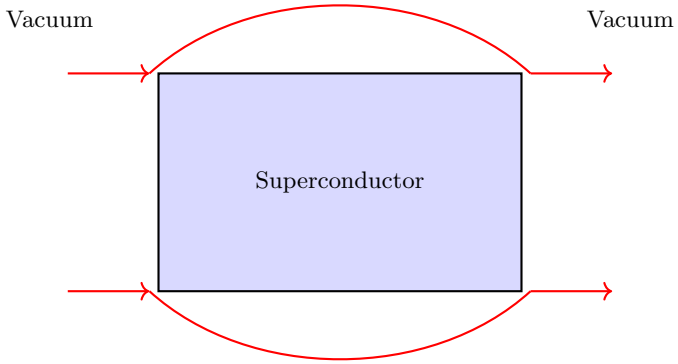

This partial exclusion (or "flux trapping") can be used to study superconductors. Let's focus on a theoretical case of hole inside a disk to understand it. With a zero field

cooling, the expected magnetic field inside the hole is zero independently how much we increase the external magnetic field. However, with a Field cooling, some field goes through the hole as it has a lower energy cost. Still, inside the SC you measure no magnetic field...

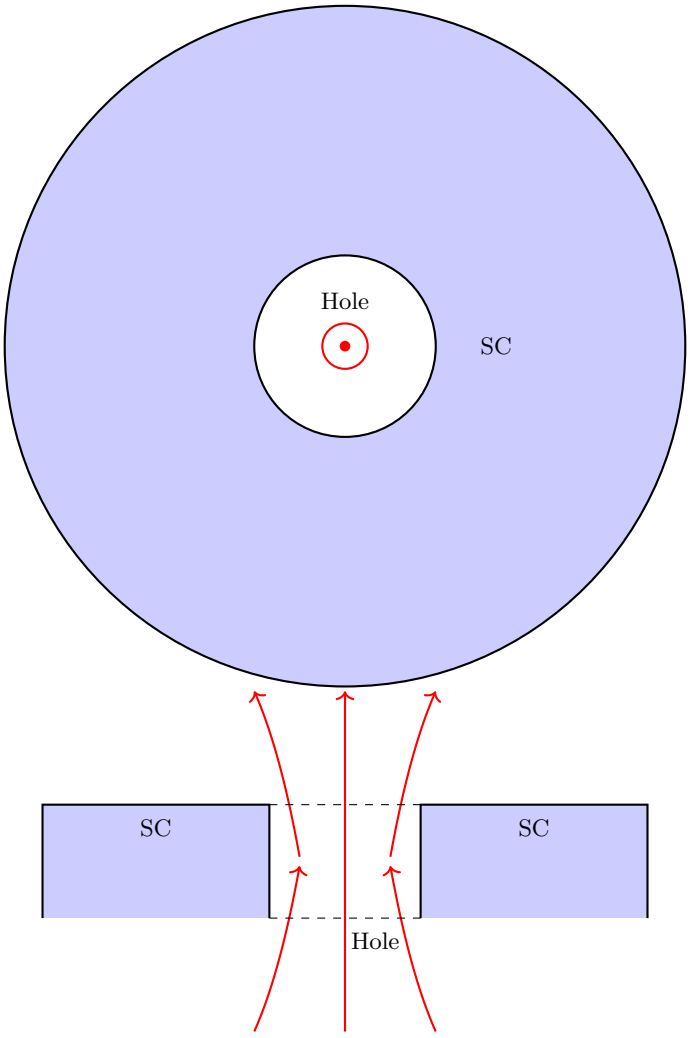

Trapped Magnetic Flux Φ when Field cooling

Question : Is the 2nd London equation indicating what could be the magnetic field in the hole ? Not at all. And then, what if change the magnetic field dynamically?

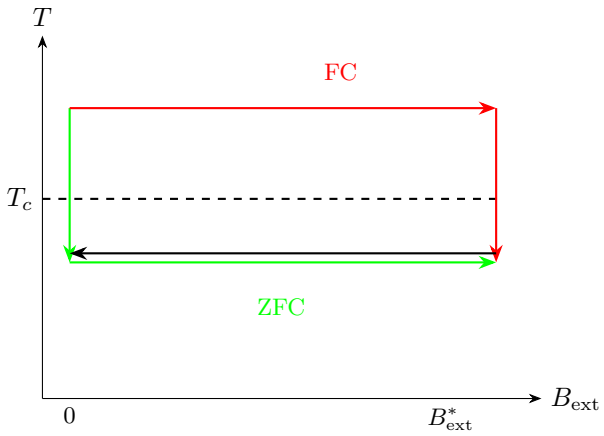

Magnetic field brought to 0 after cooling

In that configuration (black arrow), a perfect superconductor with no hole would come back to its initial state. However, with a hole inside, it would keep a magnetic field inside, or "trapped flux", which could take whatever value of B_{ext} that was inserted.

At first, two groups reported expected integer values of the magnetic flux, however, the expected Φ_0 was $\frac{hc}{e}$ as the considered charges were elecrons. The quantization was indeed observed but not at this expected values. Let's try to get an insight about what should be the magnetic flux Φ_0.

Magnetic vector potential

In the context of a superconducting loop enclosing a magnetic flux Φ, the magnetic vector potential $\mathbf{A}$ plays a central role. It is defined as :

$$\vec{B} = \boldsymbol{\nabla} \times \tilde{\mathbf{A}}$$

$$\vec{E} = -\frac{\partial \vec{A}}{\partial t}$$

This vector potantial is not unique and there is a gauge freedom of choice that gives same electric and magnetic field distribution. According to Stokes' Theorem:

$$\oint_{\mathcal{C}} \mathbf{A} \cdot \mathrm{d}\mathbf{l} = \iint_{\mathcal{S}} (\boldsymbol{\nabla} \times \mathbf{A}) \cdot \mathrm{d}\mathbf{S} = \iint_{\mathcal{S}} \mathbf{B} \cdot \mathrm{d}\mathbf{S} = \Phi \tag{4.1}$$

This relation implies that even in regions where $\mathbf{B} = 0$, the potential $\mathbf{A}$ may still be non-zero and influence the quantum phase of charged particles.

In the **Aharonov-Bohm** effect, the phase enclosed on a loop is defined as :

$$\phi_{loop} = \frac{q}{\hbar}\Phi = \frac{q}{\hbar}\oint_{\mathcal{C}} \mathbf{A} \cdot \mathrm{d}\mathbf{l}$$

If we consider the phase of a wavefunction defining our superconducting charges, we should get : $\phi_{loop} = N2\pi$. For a simply connected loop inside the superconductor, the only solution is $\phi_{loop} = 0$ everywhere and we have a well defined phase. Whenever the loop is not simply connected, $\phi_{loop} = \frac{q}{\hbar}\Phi = N2\pi$, meaning $\Phi = N\frac{h}{q}$. This flux depends only on fondamental parameters which helped to measure the ratio $\frac{h}{e}$ more precisely.

Thus, the consequence is that we have indeed quantization but it depends on the path taken and indicate that we have a state with well defined wavefunction.

The experimental value of q was determined to be $q = 2e$. The charge carrier of superconductors are not single electrons but pairs of electrons.

Generalized momentum and current operator

We define the generalized momentum such as :

$$\vec{P_G} = m\vec{v} + q\vec{A}$$

It is the conserved parameter with respect to the translation symmetry, and also the classical result, also noted :

$$K_e = \frac{(\vec{P_G} - q\vec{A})^2}{2m}$$

In quantum physics, we do write P_G as the operator $i\hbar\nabla$, so that the hamiltonian has terms in $i\hbar\nabla - qA$. Knowing this, we can get back to the current density expression. Indeed, the classical approach has some limits so let's describe the system in terms of wavefunction :

$$\Psi(x) = \langle x|\Psi\rangle = \sqrt{n_s}e^{i\phi(x)}$$

We make the approximation that the density of charge is uniform in space. The current operator is written as :

$$\vec{j} = \frac{n_s q}{m}(\hbar\nabla\phi(x) - q\vec{A})$$

which is equivalent to the 2^{nd} London equation.

Critical parameters of superconductors

Electrons not scattering is not enough to describe SC, we have to consider a "condensation" happening. Then, how to understand the critical current ? what we can tell for now is that a way to maximize the critical current is to optimize impurities and the geometry of the material.

The critical current is not the only "critical" parameter in superconductors. We also refer to the critical frequency, known as superconductive gap or optical gap. There is also a critical H field which depends strongly on the shape of the material. It is enlightening the cost of field exclusion which is roughly $\frac{H^2}{8\pi}$.

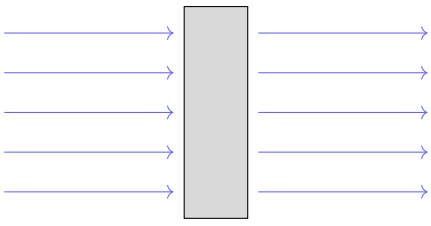

Vertical

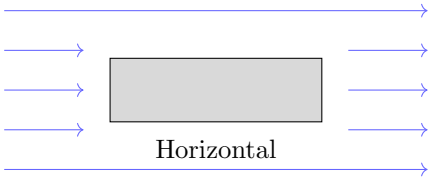

Horizontal

The horizontal orientation costs less in energy in terms of field expulsion. The thermodynamic critical field is defined as :

$$\frac{H^2_{crit}(T)}{8\pi} = f_N - f_{SC}$$

f_N is the Helmoltz free energy density of the normal phase (non SC). It follows that the critical field depends on temperature :

$$H_{crit}(T) = H_{crit}(1 - (\frac{T}{T_c})^2)$$

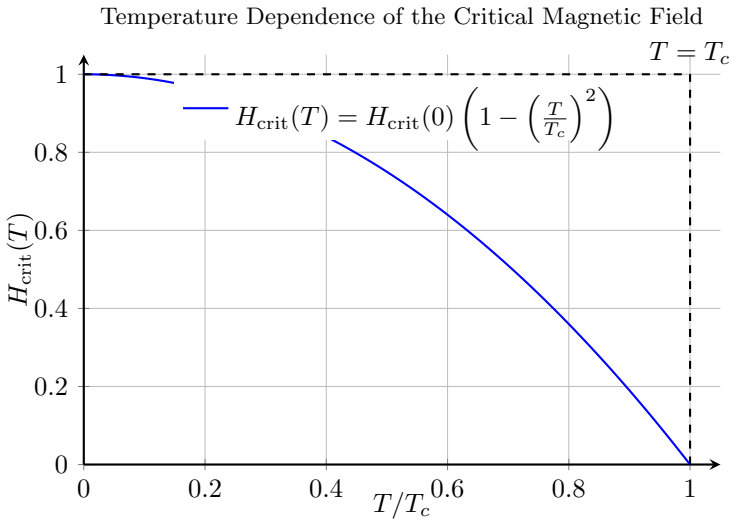

4.2.3 SQUID and flux Qubit

We now have all the ingredients to understand how some of the most interesting applications of superconductivity such as SQUIDs work. In order to explain it, let's look at the build up of a phase in superconductors which are the origin of SC currents.

Let's write the 1st London equation with the phase now:

$$\frac{\partial \phi}{\partial t} = \frac{\epsilon(x)}{\hbar} = \frac{2eV}{\hbar}$$

The phase gradient corresponds to a current, a momentum.

If we consider two classical semiconductor domains close to each others with the same charge density and let's say separated by vacuum, we wouldn't expect a current flowing in between only bringing them close together. Now, considering that they have two different but related phases, it shouldn't change anything in this simple picture. However, in a superconductor the energy would depend in the relative phase between the two, so let's try to come back to our previous two site and two level model to get a feeling about this

Bloch sphere understanding

$\rightarrow$ to finish..

Josephson equation

From the above phase-time relation and the quantum tunneling of Cooper pairs between two superconductors separated by a thin insulating barrier, we obtain the Josephson relations, here we consider any AC field (periodic function):

$$\epsilon_j = -\epsilon_0 cos(\Delta\phi)$$

then,

$$\frac{d\epsilon_j}{dt} = \epsilon_0 sin(\Delta\phi)\frac{2eV}{\hbar} = I_j V$$

where V is the imposed voltage. The derived josephson equation is :

$$I = I_c \sin(\Delta\phi)$$

Here, I_c is the critical current, typically on the order of a few **mA**, depending on the junction's geometry and materials.

Current-phase relation plot:

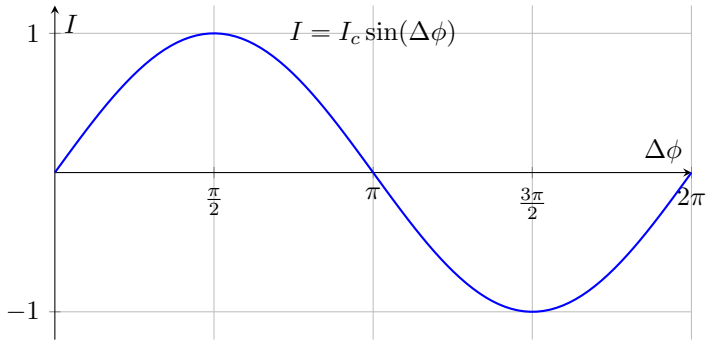

SQUID: Superconducting Quantum Interference Device

A SQUID consists of two Josephson junctions arranged in a superconducting loop. The current through the SQUID depends not only on the phase difference but also on the magnetic flux Φ threading the loop.

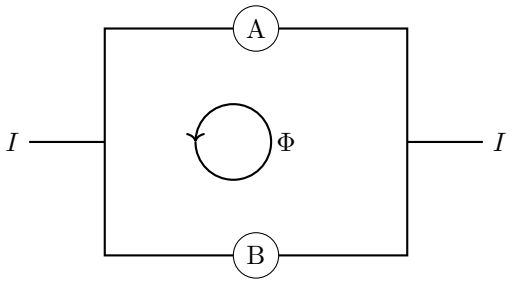

Current in a SQUID:

The total critical current of the SQUID depends on the external magnetic flux Φ and is given by:

$$I = 2I_c \cos\left(\frac{\pi\Phi}{\Phi_0}\right) \sin\left(\frac{\delta}{2}\right)$$

where $\Phi_0 = \frac{h}{2e}$ is the flux quantum and δ is the total phase difference across the junctions.

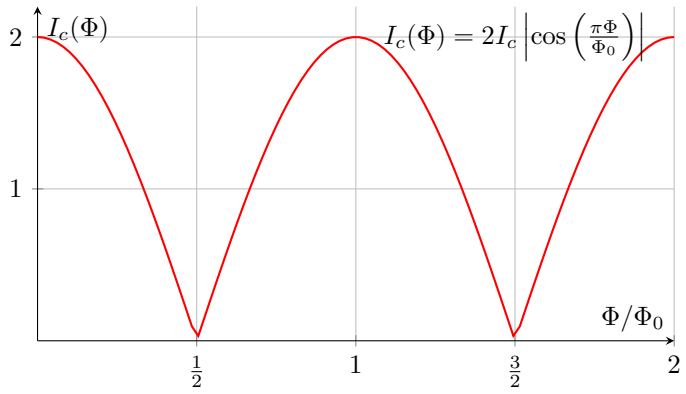

Measurement of ϕ_0 this way can be done with a precision of 10^{-18} T that helps to better define the physics constants.

4.2.4 Flux Qubit and Anharmonicity

Flux qubits are superconducting loops interrupted by Josephson junctions, typically three, that allow for the creation of two persistent current states flowing in opposite directions. These states can be used as the logical $|0\rangle$ and $|1\rangle$ of a qubit.

What makes flux qubits particularly interesting is the presence of strong **anharmonicity** in their energy spectrum. Unlike harmonic oscillators, which have equally spaced energy levels, the flux qubit has a double-well potential whose minima correspond to different current circulations. The energy levels in each well are *not* equally spaced. This anharmonicity is crucial because it allows selective addressing of transitions (e.g., $|0\rangle \rightarrow |1\rangle$) while suppressing unwanted excitations.

Nonlinearity without dissipation:

This setup is particularly remarkable because it provides a highly nonlinear response without dissipation — the Josephson effect allows currents to flow without resistance. This is in stark contrast to traditional nonlinear elements such as diodes or transistors, which are dissipative and introduce thermal noise.

This dissipation-free nonlinearity is at the heart of why superconducting circuits, including flux qubits and Josephson parametric amplifiers, are so powerful for low-noise applications such as quantum information processing and quantum-limited amplification.

4.2.5 Flux Trapping in a Ring-Shaped Superconductor

Now, we consider a superconducting ring and examine what happens during cooling in the presence of an external magnetic flux. It is well known that flux quantization can occur — but how is this consistent with zero resistivity and no voltage?

Qualitative argument:

As the ring cools down below the critical temperature in the presence of a magnetic field, it transitions into the superconducting state. Due to flux quantization, the total magnetic flux inside the ring must equal an integer multiple of the flux quantum $\Phi_0 = h/2e$. However, since superconductors tend to expel magnetic fields (Meissner effect), the only way to preserve this quantization while canceling the external field is by inducing a persistent current in the ring.

But here's the subtle point: even though there's a current, it doesn't necessarily flow *everywhere* in the ring. There must be at least one path — a point or region — where the current density is zero. Otherwise, we wouldn't have a consistent solution for the supercurrent around a closed loop with a quantized phase.

Quantum mechanical derivation:

Let's formalize this using the Schrödinger equation. We consider a superconducting ring and write the wavefunction of the superconducting condensate in the **Coulomb gauge**, assuming no scalar potential $V = 0$ and vector potential $\vec{A} \neq 0$. The wavefunction can be decomposed in a Fourier series along the ring coordinate θ:

$$\Psi(\theta) = \sum_n c_n e^{in\theta}$$

In the Coulomb gauge, the minimal coupling Hamiltonian for a charged particle in a vector potential is:

$$\hat{H} = \frac{1}{2m}\left(-i\hbar\nabla - q\vec{A}\right)^2$$

On a ring of radius R, the kinetic energy becomes:

$$E_n = \frac{1}{2mR^2}\left(\hbar n - qA_\theta R\right)^2$$

The energy is minimized when the quantity inside the square is closest to zero. This happens when:

$$\hbar n - qA_\theta R = 0 \quad \Rightarrow \quad n = \frac{qRA_\theta}{\hbar}$$

Since the phase ϕ must be single-valued around the ring (i.e., $\Psi(\theta + 2\pi) = \Psi(\theta)$), we require $n \in \mathbb{Z}$, leading to the quantization of the total flux:

$$\Phi = \oint \vec{A} \cdot d\vec{l} = n\frac{h}{q}$$

For Cooper pairs with charge $q = 2e$, this becomes:

$$\Phi = n\Phi_0, \quad \Phi_0 = \frac{h}{2e}$$

This confirms that flux quantization is a natural consequence of minimizing the energy of a periodic superconducting wavefunction.

Zero current density path:

If you plot the supercurrent density $j(\theta) \propto |\Psi(\theta)|^2 \nabla\phi$, and the total current satisfies the quantization condition, then at least one point along the ring must satisfy $j(\theta) = 0$ — to accommodate the flux quantization without violating continuity or introducing discontinuity in the phase.

4.2.6 Vortices and Ginzburg-Landau Theory

To describe superconductors on a macroscopic scale — including the formation of vortices — we now introduce the **Ginzburg-Landau (GL) theory**. The GL free energy functional involves a complex order parameter $\psi(\vec{r})$, which represents the local density of Cooper pairs.

The GL equations are derived by minimizing the free energy:

$$F = \int d^3r \left[\alpha|\psi|^2 + \frac{\beta}{2}|\psi|^4 + \frac{1}{2m^*} \left| \left(-i\hbar\nabla - q\vec{A} \right) \psi \right|^2 + \frac{|\vec{B}|^2}{2\mu_0} \right]$$

Minimizing this functional yields the Ginzburg–Landau equation:

$$\frac{1}{2m^*} \left| \left(-i\hbar\nabla - q\vec{A} \right) \psi \right|^2 + \alpha\psi + \beta|\psi|^2\psi = 0$$

From this equation, two important physical length scales can be defined:
- The **coherence length**:

$$\xi = \sqrt{\frac{\hbar^2}{2m^*|\alpha|}}$$

- The **London penetration depth** (reintroduced when $\vec{A} \neq 0$):

$$\lambda = \sqrt{\frac{m^*}{\mu_0 q^2 |\psi_\infty|^2}}, \quad \text{with } |\psi_\infty|^2 = -\frac{\alpha}{\beta}$$

The Ginzburg-Landau parameter:

$$\kappa = \frac{\lambda}{\xi}$$

This dimensionless number determines the type of superconductor:
- $\kappa < \frac{1}{\sqrt{2}}$: **Type I superconductor**, exhibits complete Meissner effect and sharp transition into the normal state.
- $\kappa > \frac{1}{\sqrt{2}}$: **Type II superconductor**, allows partial magnetic penetration via quantized **vortices** above a lower critical field H_{c1} and below an upper critical field H_{c2}.

Sketch of the vortex:
The vortex solution appears when the phase of the order parameter winds by 2π around a point, and the modulus $|\psi|$ vanishes at the center.

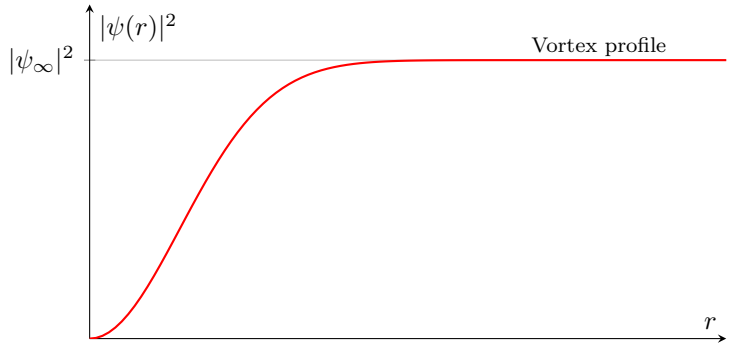

At the core $r = 0$, the order parameter vanishes: $|\psi(0)| = 0$. It recovers to its bulk value $|\psi_\infty|^2 = -\alpha/\beta$ over a length scale ξ. Circulating supercurrents (not shown here) would appear if a vector potential $\vec{A}$ were included.

These vortices can form a lattice and play a crucial role in the mixed state of type II superconductors.

4.2.7 A little bit about Condensation and Pairing in Superconductors

Before going further into vortex dynamics and topological effects, let's step back and ask: *What actually condenses in a superconductor?*

In most conventional superconductors, the condensation temperature — the temperature below which a macroscopic quantum state forms — is **much higher** than the temperature at which electron pairs (Cooper pairs) actually form. This indicates that pairing happens first, and condensation occurs when these pairs begin to behave collectively in a coherent quantum state.

Why do electrons pair at all?

Electrons repel each other via Coulomb interaction, so naively, pairing seems unlikely. However, in the solid-state environment, this repulsion is effectively reduced due to interactions with the positively charged ion lattice.

In a simplified picture, when an electron moves through the lattice, it slightly distorts the ion positions — attracting them and creating a local positive region. A second electron can then be attracted to this distortion. This mechanism, mediated by **phonons**, leads to an effective attraction between electrons at low energies and long distances.

Standing wave and energy lowering — BCS perspective:

When we consider the quantum wavefunctions of electrons near the Fermi surface, the formation of standing wave-like superpositions of momenta ($\vec{k}$ and $-\vec{k}$) becomes energetically favorable. In the BCS theory, this superposition leads to a **collective potential well**, which lowers the total energy of the system compared to the normal state.

The condensation of these pairs into a macroscopic quantum state — with a single phase and a well-defined gap — is what defines the superconducting phase.

This opens the door to today's research directions:

- What are the limits of phonon-mediated pairing? - Can other mechanisms (spin fluctuations, topological effects, moiré structures) give rise to high-T_c or unconventional superconductivity? - How do we model and control the collective condensate for quantum technologies?

These questions drive much of the ongoing research in condensed matter and quantum materials today.